# Multiattribute Decision-making in Macaques Relies on Direct Attribute Comparisons

**Aster Q. Perkins[1], Zachary S. Gillis[1,2], and Erin L. Rich[1]**

## Abstract

■ In value-based decisions, there are frequently multiple attributes, such as cost, quality, or quantity, that contribute to the overall goodness of an option. Because one option may not be better in all attributes at once, the decision process should include a means of weighing relevant attributes. Most decision-making models solve this problem by computing an integrated value, or utility, for each option from a weighted combination of attributes. However, behavioral anomalies in decision-making, such as context effects, indicate that other attribute-specific computations might be taking place. Here, we tested whether rhesus macaques show evidence of attribute-specific processing in a value-based decision-making task. Monkeys made a series of decisions involving choice options comprising a sweetness and probability attribute. Each attribute was represented by a separate bar with one of two mappings between bar size and the magnitude of the attribute (i.e., bigger = better or bigger = worse). We found that translating across different mappings produced selective impairments in decision-making. Choices were less accurate and preferences were more variable when like attributes differed in mapping, suggesting that preventing monkeys from easily making direct attribute comparisons resulted in less accurate choice behavior. This was not the case when mappings of unalike attributes within the same option were different. Likewise, gaze patterns favored transitions between like attributes over transitions between unalike attributes of the same option, so that like attributes were sampled sequentially to support within-attribute comparisons. Together, these data demonstrate that value-based decisions rely, at least in part, on directly comparing like attributes of multiattribute options. ■

## INTRODUCTION

Complex, real-world decisions often do not have a clear best option. This is because there are typically multiple relevant features, or attributes, such as quantity, quality, or cost, that need to be considered to select the most preferred combination. This process could evolve in different ways, and it remains unclear how the brain uses information about different attributes to compute these types of complex decisions.

A canonical solution to this problem is to compute an integrated value, or utility, for each option from a weighted combination of all relevant information. This could allow different options to be compared on a common scale, accounting for context, internal state, and different features or attributes of unalike options (Padoa-Schioppa, 2011; Wallis & Rich, 2011; Rangel & Hare, 2010; Glimcher, Dorris, & Bayer, 2005). Many views have proposed that decision computation occurs by comparing these integrated option values (Figure 1A; Rustichini & Padoa-Schioppa, 2015; Hunt et al., 2012). Neural responses correlating with variables in these models have been widely reported (Hunt, Behrens, Hosokawa, Wallis, & Kennerley, 2015; Jocham, Hunt, Near, & Behrens, 2012; Padoa-Schioppa & Assad, 2006; Wallis & Miller, 2003; Tremblay & Schultz, 1999), supporting the idea that the brain is capable of computing something like integrated value.

In contrast, behavioral anomalies that are inconsistent with the "integrate then compare" model of decision-making are also well documented (Piantadosi & Hayden, 2015; Brandstätter, Gigerenzer, & Hertwig, 2006; Stewart, Chater, & Brown, 2006; Simonson, 1989; Huber, Payne, & Puto, 1982; Kahneman & Tversky, 1979) and suggest that integrated value may not be the sole input into the decision process. For instance, choice biases known as "decoy" or context "effects" arise when third options are added to the choice set (Simonson, 1989; Huber et al., 1982; Kahneman & Tversky, 1979). In these cases, the direction of the bias depends on where the third option's attributes are situated with respect to those of the other options. A suite of conceptual and quantitative decision-making models have been developed to explain these empirical results. Although there is heterogeneity in this family of models, a common feature is that they include comparisons at the level of individual attributes, either alone or in addition to comparisons of integrated values (Figure 1B and C; Piantadosi & Hayden, 2015; Brandstätter et al., 2006; Stewart et al., 2006; although see Chau, Law, Lopez-Persem, Klein-Flügge, & Rushworth, 2020; Gluth,

[1]Icahn School of Medicine at Mount Sinai, NY, [2]Wake Forest University School of Medicine, NC



Journal of Cognitive Neuroscience 36:9, pp. 1879–1897
https://doi.org/10.1162/jocn_a_02208

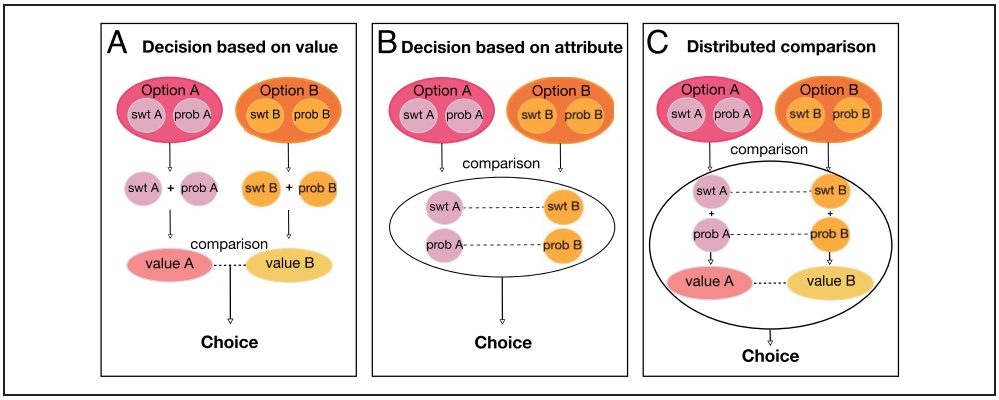


**Figure 1.** Three models of goal-directed decision-making. Each box shows a representative two-option choice. As in our task, each option (A and B) consists of two attributes: sweetness (swt) and probability (prob). (A) In the "integrate then compare" model, attributes are combined to compute an integrated value for each option, which is then compared to the other option's value to produce a decision. (B) An attribute comparison model, in which like features (attributes) are compared directly, so that the number and weight of each competition in favor of an option produce a choice. (C) A hybrid model, in which comparisons occur at the multiple levels, including comparisons of attributes and integrated values, so that decisions arise from distributed processes. (Adapted from Perkins & Rich, 2021.)

Kern, Kortmann, & Vitali, 2020; Gluth, Spektor, & Rieskamp, 2018; Chau, Kolling, Hunt, Walton, & Rushworth, 2014; Louie, Khaw, & Glimcher, 2013). For instance, decision field theory accounts for context effects by eschewing models that rely on overall utility and instead suggesting that preferences evolve over the course of a decision by incorporating a continuous stream of comparisons of attributes (Roe, Busemeyer, & Townsend, 2001; Busemeyer & Townsend, 1993). Options are represented in a multi-attribute preference space and can interact, such that closely related options compete with one another to influence choice, with attention fluctuations determining the relative weights of different attributes in the decision.

A related view is taken by attentional drift diffusion models (aDDMs; Krajbich & Rangel, 2011; Basten, Biele, Heekeren, & Fiebach, 2010; Krajbich, Armel, & Rangel, 2010; Milosavljevic, Malmaud, Huth, Koch, & Rangel, 2010; Philiastides, Biele, & Heekeren, 2010), including recent multiattribute instantiations (Yang & Krajbich, 2022; Fisher, 2017, 2021), which model decisions as a noisy process of accumulating evidence over time, until a threshold is reached and finalizes the choice. aDDMs have become a popular model of value-based decision-making because they account for the effects of attention, which influences both choice and neural encoding of values of visually attended items (Smith & Krajbich, 2019; Hunt et al., 2018; McGinty, Rangel, & Newsome, 2016; Krajbich et al., 2010). The multiattribute aDDM makes the assumption that like attributes are directly compared while the options are also directly compared, each feeding into the overall decision. Notably, there is no one "integrated value," only an accumulation of evidence.

Another view suggests that integrated values are computed and compared, and this occurs in parallel with attribute-level comparisons (Figure 1C). In the distributed theory of decision-making, decisions are an emergent property of computations performed in multiple brain regions (Hunt & Hayden, 2017; Hunt, Dolan, & Behrens, 2014; Cisek, 2012). Therefore, competitions among different choices occur at multiple levels of representation, including offer values, goals, and actions. Regions share information in an ordered way but do not represent a circuit in the canonical sense. Rather, recurrent and overlapping computations are spread across the brain and produce choice through their interactions. A specific instantiation of this model proposes direct competition, via mutual inhibition, at the level of attributes as well as options, with each feeding into option-level accumulators that compete with each other and produce a decision output (Hunt et al., 2014). In this way, both attribute and option comparisons contribute to choices in a hierarchical fashion. Collectively, these models represent alternatives to utility-based explanations of choice behavior and demonstrate that the mechanism of preference-based decision-making is far from a solved matter.

Here, we explored the potential for direct interaction or comparison between attributes by analyzing multiattribute decision-making behavior in rhesus macaques. The monkeys were trained to choose between options that varied in the sweetness of a sugar water reward and the likelihood of receiving it. Each attribute was represented by visually distinct bars whose sizes changed with respect to the sweetness and probability level. Critically, bars were presented in two mappings denoted by different colors: one in which the size changed proportional to the goodness of the attribute (i.e., "bigger is better") and one in which the size changed inversely proportional to the goodness of the attribute ("bigger is worse"). Both attribute magnitude and mapping varied independently, allowing us to reveal consistent patterns of choice deficits that indicated the spontaneous use of within-attribute comparisons, even when all information was available to compute integrated values. Therefore, comparisons between individual attributes of multiattribute options appear to be a natural feature of goal-directed decision-making in monkeys. This result opens new questions about the neural mechanisms underlying complex, goal-directed decisions.

## METHODS

### Experimental Design

We used a multiple attribute decision-making task to test whether the choices of rhesus macaques are consistent with comparing integrated values or like attributes to make decisions.

#### *Subjects and Behavior*

Two adult male rhesus macaques ("C" and "D") participated in the experiment. Neither animal had been used for previous studies; however, they had been trained on a battery of tasks. They were each 5 years old and weighed 11.8 and 9.4 kg, respectively, at the start of experiments. Each was surgically implanted with a titanium head positioner. All procedures were in accord with the National Institutes of Health guidelines and were approved by the Icahn School of Medicine at Mount Sinai Animal Care and Use Committee.

During experiments, monkeys sat in a primate chair in a darkened testing chamber and were head-fixed facing an 18-in. computer monitor positioned 17 in. away from the subjects' faces. MonkeyLogic software (Hwang, Mitz, & Murray, 2019; Yiu et al., 2019; Asaad, Santhanam, McClellan, & Freedman, 2013) controlled the behavior interface. Subjects' eye position was continuously monitored by an infrared eye tracker (ViewPoint EyeTracker USB-400, Arrington Systems) at a sampling rate of 400 Hz. This signal was acquired by MonkeyLogic at 500 Hz to align to behavioral data.

#### *Task*

Each trial began with the appearance of a fixation cue in the center of the screen. When the monkey gazed at the fixation point and simultaneously held a touch-sensitive bar for 550 msec, two (80% of trials) or three (20% of trials) choice options were displayed on the screen. Options were shown at two or three of six potential positions in a hexagonal arrangement around central fixation. Option positions were selected randomly, with the constraint that they were never in adjacent positions on the hexagon. Only two-option trials were analyzed in the present study.

Options were presented as a set of two bars. The width of each bar was 2° of visual angle, and the height varied from 2° to 10°. The size of the left bar of each pair indicated the sweetness level (25-, 50-, 75-, 100-, or 125-mM sucrose solution), whereas the right bar represented the probability level (10%, 30%, 50%, 70%, or 90%). The colors of the bars indicated whether the size of the bar positively correlated with sweetness/probability level, referred to as "direct mapping," or negatively correlated with sweetness/probability level ("indirect mapping"). For example, a blue sweetness bar indicated a direct mapping (large bar = high sweetness), whereas a magenta sweetness bar indicated an indirect mapping (large bar = low sweetness). Bar size and mapping varied randomly and independently on each trial.

While the monkeys continued to hold the touch bar, they had up to 5 sec to freely view the images while gaze position was tracked. They could make a selection at any time by holding gaze on any part of the desired option and releasing the touch-sensitive bar. This would trigger the reward delivery immediately after an option was selected. If an option was not selected in this window, or if the touch bar was released when gaze was not directed toward an option, this triggered a 5-sec timeout, during which no reward was delivered and the screen displayed a red background. When the timeout was complete, the next trial could be initiated. Intertrial intervals were 1 sec.

Rewards consisted of 0.33 mL of fluid delivered over 500 msec for Monkey D and 0.297 mL delivered over 450 msec for Monkey C. Different amounts were titrated during pretraining to account for each subject's relative weighting of sweetness and probability, to balance as closely as possible their subjective preference between the two attributes.

### Statistical Analysis

The number of subjects was not predetermined by any statistical methods. Two animals is a common standard for monkey experiments because it is the smallest number with which we can demonstrate reproducibility. All of our analyses were carried out within subject, so that the $n$ for statistical tests is the number of trials or sessions. The same analyses were then carried out as replications in the second animal. The number of trials and sessions is within the range of previous literature (Yamada, Imaizumi, & Matsumoto, 2021; Padoa-Schioppa & Assad, 2006).

Some trials were excluded because the animal failed to make a choice within 5 sec (Monkey D: 599, 1.04%, Monkey C: 1203, 1.8%). There were more omissions on trials with a smaller difference in values (i.e., more difficult trials). In addition, three-option trials were part of the task design but were excluded for the analyses in this article. All statistical analyses were conducted with custom MATLAB (The MathWorks Inc.) scripts.

#### *Accuracies and RTs*

Accuracies were calculated as the number of trials in which the option with the highest expected value (EV; defined as ordinal sweetness level multiplied by ordinal probability level) was selected over other options, divided by the number of valid trials in the same category. Because this calculation relies on assumptions about how the attributes are weighed by the subjects, we also computed accuracies for a subset of "objective" trials, in which one option had higher values of both sweetness and probability than the other (e.g., SwtA > SwtB and ProbA > ProbB), meaning it was the superior option regardless of attribute weighting. RTs were measured as the time from stimulus onset to

release of the touch bar, indicating option selection. For Figure 3B, two 2-tailed binomial tests were performed between the "all consistent" group and the "different within option" group and between the "all consistent" group and the "different within attribute" group (Nelson, 2023). Significance levels were Bonferroni-corrected for multiple comparisons to $\alpha = .005$.

### *Choice Regressions*

We used the choice behavior of each monkey to examine the influence of task variables on decision-making. To quantify how each monkey weighs sweetness and probability, choices were modeled as a function of the log ratio of each attribute (Conen & Padoa-Schioppa, 2019; Padoa-Schioppa & Assad, 2008):

$$\begin{aligned} X = {} & \beta_0 + \beta_{\text{Prob}}\left(log\frac{ProbA}{ProbB}\right) + \beta_{\text{Swt}}\left(log\frac{SwtA}{SwtB}\right) \\ & + \beta_{\text{SwtDirA}}SwtDirA + \beta_{\text{SwtDirB}}SwtDirB \\ & + \beta_{\text{ProbDirA}}ProbDirA + \beta_{\text{ProbDirB}}ProbDirB \\ & + \beta_{\text{PositionA}}PositionA + \beta_{\text{PositionB}}PositionB \end{aligned} \quad (1)$$

Options were arbitrarily designated "A" and "B." *ProbA* or *B* and *SwtA* or *B* are the ordinal magnitudes of probability and sweetness, respectively, available in each option. $\beta_{\text{prob/Swt}}$ are fitted weights of probability/sweetness attributes. *(Prob/Swt)Dir(A/B)* is the mapping for each attribute bar, coded as $-1$ or 1, with the corresponding coefficient ($\beta_{\text{(prob/Swt)Dir(A/B)}}$). *Position(A/B)* is the position index (1–6) indicating one of six sites where options are presented on the screen, and $\beta_{\text{position(A/B)}}$ is the corresponding coefficient. Only overall option locations were included because the two attributes of an option were always proximal to each other on the screen. $\beta_0$ is a constant to capture any bias toward A or B. The probability of choosing option A was then calculated by a sigmoid function (Equation 2).

$$\Pr(ChoiceA) = {}^{1}\Big/{(1 + e^{-x})} \quad (2)$$

Choice probability colormaps were created from interpolating choice probabilities from the logistic regression on choice data, as above. Regressions were performed on concatenated data from all sessions, although session-by-session performance on each regression was assessed and is noted where included.

To perform the bootstrap analysis in Figure 3C, we reduced Equation 1 to just sweetness and probability ratios, as there were limited effects of the additional predictors in the original model:

$$X = \beta_0 + \beta_{\text{Prob}}\left(log\frac{ProbA}{ProbB}\right) + \beta_{\text{Swt}}\left(log\frac{SwtA}{SwtB}\right) \quad (3)$$

Equation 3 was then used with Equation 2 to perform the bootstrapped logistic regression.

### *RT Regression*

To quantify how task variables affected RTs, a general linear regression was performed on concatenated data from all sessions.

$$\begin{aligned} log(ReactionTime) = {} & \beta_0 + \beta_{\text{SwtDiff}}SwtDiff \\ & + \beta_{\text{ProbDiff}}ProbDiff + \beta_{\text{NumSwtInd}}NumSwtInd \\ & + \beta_{\text{NumProbInd}}NumProbInd \end{aligned} \quad (4)$$

*SwtDiff* denotes the difference in the ordinal sweetnesses of the two options (0–4), and *ProbDiff* denotes the difference in the ordinal probabilities of the two options (0–4). *NumSwtInd* denotes the number of sweetness bars with the indirect mapping (0–2); *NumProbInd* denotes the number of probability bars with the indirect mapping (0–2). All predictors were mean centered (ranges above are before mean centering).

### *Gaze Data Analysis*

Gaze analyses were done with the EyeMMV MATLAB package (Krassanakis, Filippakopoulou, & Nakos, 2014), which extracts fixations from continuous eye movements. Minimum fixation duration was set as 50 msec, a liberal criterion that allowed us to capture shorter fixations as assessed by visual inspection (Berg, Boehnke, Marino, Munoz, & Itti, 2009). Tolerances were set as $t_1 = 2$ and $t_2 = 1$, where $t_1$ was the criterion in Euclidean distance within which gaze track records would be included in a fixation cluster and $t_2$ was the criterion in Euclidean distance within which gaze track records would be included in the computation of a fixation cluster mean. ROIs were then defined to include each attribute bar in a session, and fixations falling on each attribute were retained for analysis. The eye tracker was calibrated at the start of each session, and gaze data were further aligned in postprocessing by centering data to the median $x - y$ coordinates for the initial fixation window (placing it at the center fixation cue) across the session. In addition, ROIs around each attribute bar used for fixation detection were expanded by 0.75° of visual angle on the outside of the bars and 0.5° of visual angle on the inside (so that there was no unassigned space between the bars), to capture fixations that were on the bar edges. Likewise, 0.5° of visual angle was added to the top and bottom of the ROIs.

Unless otherwise stated, analyses were performed on fixations that occurred between option presentation and choice. Fixations detected immediately after option presentation were still at the center fixation cue and were eliminated by removing all fixations beginning in a 50-msec window after the stimulus presentation. The final fixation in the choice window was the fixation of the chosen option and was also eliminated by removing the last fixation in the response window. Ultimately, 14,030 trials in Monkey D (24.6%) and 26,603 trials in Monkey C (40.7%) were excluded from prechoice analyses for having no prechoice fixations.

*Regressions on Number of Fixations*

To quantify the effects of task variables on the number of fixations in each trial, we used a linear regression model as follows:

$$\begin{aligned} NumberFixations = {} & \beta_0 + \beta_{SwtDiff} SwtDiff \\ & + \beta_{ProbDiff} ProbDiff + \beta_{NumSwtInd} NumSwtInd \\ & + \beta_{NumProdInd} NumProdInd \end{aligned} \quad (5)$$

where *SwtDiff* represents the difference between the sweetnesses of the two options (0–4), *ProbDiff* represents the difference between the probabilities of the two options (0–4), *NumSwtInd* represents the number of sweetness bars that were indirect (0–2), and *NumProbInd* represents the number of probability bars that were indirect (0–2). All predictors were mean centered (ranges above are before mean centering).

*Regression on Fixation Duration*

To quantify the effects of task variables on the duration of fixations, we used a linear regression model as follows:

$$\begin{aligned} log(Fixation\ Duration) = {} & \beta_0 + \beta_{Swt|Prob} Swt|Prob \\ & + \beta_{Ch|Unch} Ch|Unch + \beta_{Dir|Ind} Dir|Ind \\ & + \beta_{FixVal} FixVal + \beta_{OtherAttSameOpt} OtherAttSameOpt \\ & + \beta_{SameAttOtherOpt} SameAttOtherOpt \\ & + \beta_{OtherAttOtherOpt} OtherAttOtherOpt \\ & + \beta_{Swt|Prob*FixVal} Swt|Prob * FixVal \\ & + \beta_{Ch|Unch*FixVal} Ch|Unch * FixVal \\ & + \beta_{Dir|Ind*FixVal} Dir|Ind * FixVal \end{aligned} \quad (6)$$

where *Swt*|*Prob* represents whether the fixated bar was for sweetness or probability (1, −1), *Ch*|*Unch* represents whether the fixated bar was part of the chosen or unchosen option (1, −1), *Dir*|*Ind* represents whether the fixated bar was the direct or indirect mapping (1, −1), and *FixVal* represents the attribute value of the fixated bar (1–5). *OtherAttSameOpt* represents the ordinal magnitude of the other attribute of the same option as the fixated bar (1–5), *SameAttOtherOpt* represents the ordinal magnitude of the same attribute as the fixated bar in the other option (1–5), and *OtherAttOtherOpt* represents the ordinal magnitude of the other attribute of the other option as the fixated bar (1–5). All predictors were mean centered (ranges above are before mean centering).

*Hypothesis Test on Regression Coefficients for Gaze Transitions*

Value difference was regressed against the number of gaze transitions in two simple regressions. The first ($\beta_{within\ att}$) predicted the number of within-attribute gaze transitions within a trial (e.g., *SwtA* ↔ *SwtB*), and the second ($\beta_{within\ opt}$) predicted the number of within-option gaze transitions within a trial (e.g., *SwtA* ↔ *ProbA*). The *t* statistic for the two-sample hypothesis test that the slopes of these regressions differed was calculated as

$$t = \frac{\left(\beta_{within\ att} - \beta_{within\ opt}\right)}{\sqrt{SE^2_{within\ att} + SE^2_{within\ opt}}} \quad (7)$$

where *SE* is the standard error of the regression coefficient (Zaiontz, n.d.).

*Choice Models*

The probability of choosing an arbitrary option A was fit by generalized linear models with the logit link function (Equation 2). This is equivalent to obtaining a softmax decision rule (Sutton & Barto, 2018) that probabilistically selects the option with the higher value. For the purposes of this analysis, models were simplified to include only information about attribute magnitudes, not mappings. Three models differed only in how attributes were combined.

The Log model was the same as Equation 3, and fit choices based on the log ratio of each attribute:

$$X = \beta_0 + \beta_{Prob}\left(log\frac{ProbA}{ProbB}\right) + \beta_{Swt}\left(log\frac{SwtA}{SwtB}\right) \quad (8)$$

The difference (Diff) model parameterized each attribute independently, resulting in a linear combination of attributes:

$$\begin{aligned} X = {} & \beta_0 + \beta_{ProbA}(ProbA) + \beta_{SwtA}(SwtA) \\ & + \beta_{ProbB}(ProbB) + \beta_{SwtB}(SwtB) \end{aligned} \quad (9)$$

The EV model first computed EVs of each option as the direct multiplication of probability and milligrams of sucrose (Suc) and then fit choices based on the EVs available on each trial:

$$X = \beta_0 + \beta_A(ProbA * SucA) + \beta_B(ProbB * SucB) \quad (10)$$

We compared the models as follows: First, coefficient weights in each model were obtained by fitting monkeys' behavior, separately for each session. Model fits to behavior were compared with Akaike information criteria (AICs), and the relative likelihood of each model was computed as follows:

$$e\frac{AIC_{min} - AIC_i}{2} \quad (11)$$

where $AIC_i$ is the *AIC* value obtained from the *i*th model and $AIC_{min}$ is the minimum *AIC* across the three models.

Optimality of each model was then tested by using the fitted models to predict choices on all 625 possible comparisons of different combinations of sweetness and probability. Expected rewards for these choices were calculated by adding the probability of selecting option A times the EV of A (in milligrams of sucrose) plus the probability of selecting option B times the EV of option B.

Finally, the performance of models fit to actual choice data was compared to that of the same models fit to simulated choices, where the choice options were drawn from the actual sessions, but the simulated choice corresponded to the option with the higher EV, calculated for each option as *Prob * Suc*. The fits of each model to these simulated choices were again compared with AICs and relative model likelihoods as above.

## RESULTS

### Monkeys Use Multiple Attributes to Make Optimal Choices

Two monkeys performed a decision-making task in which they selected between options comprising two attributes: the sucrose concentration of a fluid reward ("sweetness") and the probability that it would be delivered ("probability"; Figure 2A). Attributes varied across five magnitudes, denoted by the length of separate bars. Bar size varied either directly (i.e., bigger is better) or indirectly (i.e., bigger is worse) with the magnitude of sweetness or probability, and the mapping was denoted by the bar color (Figure 2B). For example, a large blue bar would indicate a sweeter option, whereas a large magenta bar would indicate a less sweet option. Sweetness and probability magnitudes and mappings varied independently in both options, and pairs of bars composing an option were pseudorandomly assigned to one of six possible locations on the task screen. To initiate a trial, subjects held a touch-sensitive bar while fixating a central point. Two options were shown, each consisting of two bars. Monkeys freely viewed the options and made a choice by releasing the bar while holding gaze on one option. Reward was probabilistically delivered, depending on the option selected. We quantified choice behavior from 57,082 and 65,384 trials for Monkeys D and C, respectively, performed over 69 and 76 sessions.

Both monkeys performed the task well and often chose the option with the highest EV, when this was defined as the product of sweetness and probability (across sessions: Monkey D, 0.81 ± 0.007 [95% CI]; Monkey C, 0.82 ± 0.006 [95% CI]). Subjects chose the higher value option slightly less frequently on trials where all attribute mappings were indirect, compared to when they were all direct (across sessions: Monkey D: direct: 0.84 ± 0.013 [95% CI], indirect: 0.81 ± 0.02 [95% CI]; Monkey C: direct: 0.84 ± 0.013 [95% CI], indirect: 0.80 ± 0.013 [95% CI]). However, this effect was small, and monkeys still performed at a high level for both mappings, demonstrating that they are capable of using both mappings flexibly to retrieve information about the different attributes.

Because this definition of EV does not account for subjective preferences that differentially weight sweetness or

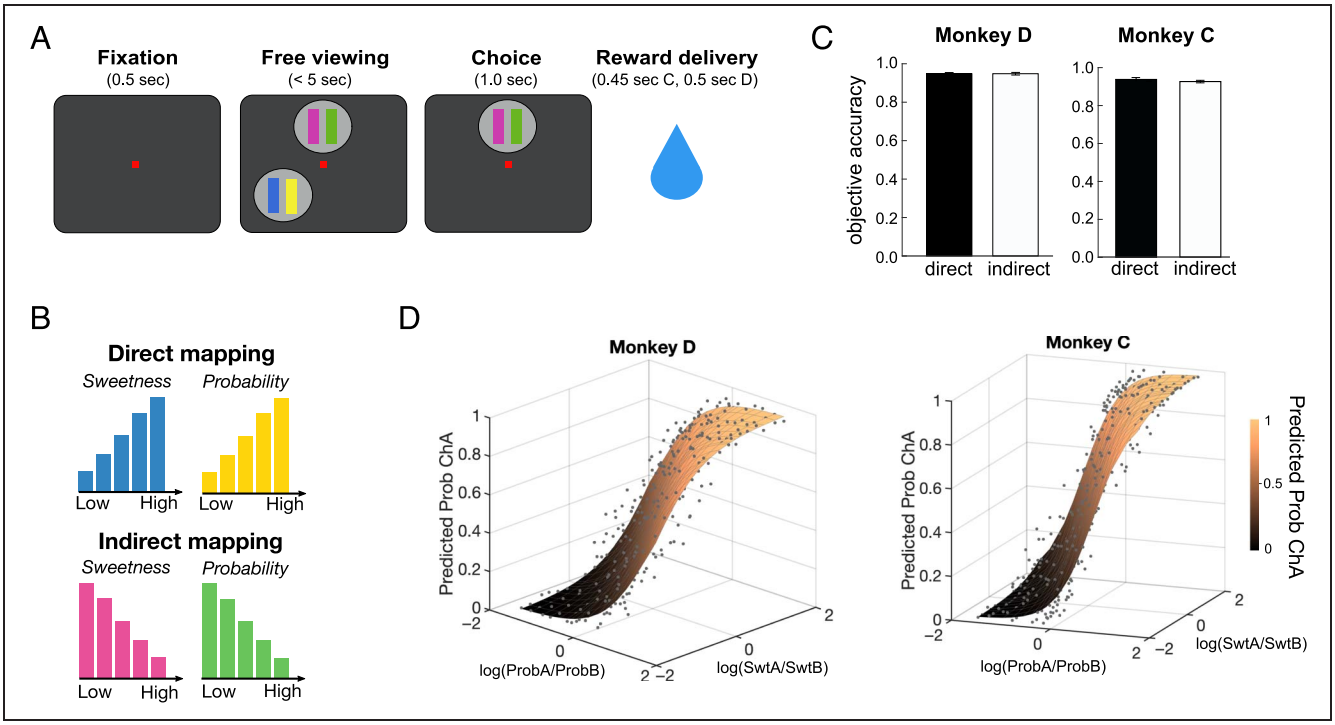


**Figure 2.** Multiattribute choice task and performance. (A) Trial schematic, where each option consists of a pair of bars indicating sweetness (left) and probability (right). The figure shows two of six possible option locations. After the monkey makes a selection, the unchosen option disappears, and reward is probabilistically delivered. (B) Each attribute bar had one of two mappings. Blue/yellow indicated a direct mapping, in which taller bars represented greater sweetness/probability. Magenta/green indicated an indirect mapping, in which taller bars represented lower sweetness/probability. (C) Accuracy based on EV in "objective trials," split by direct and indirect mapping. Error bars indicate *SEM*. (D) Interpolated predictions from fitted models (surfaces) show that the probability of choosing an arbitrary option A (Prob ChA) increases as the relative sweetness or probability of that option increases, and the attributes contribute roughly equally to decisions (Equation 3). Actual choice frequencies (points) are well fit by the model. Monkey D: $n$ = 57,082; Monkey C: $n$ = 65,384.

probability, we also calculated objective accuracy on trials where one option was superior in both sweetness and probability. This excluded trials in which one option was greater in one attribute but lower in the other (note that this is irrespective of mappings). Objective accuracies were very high, likely reflecting the fact that these were easier decisions (Figure 2C; across sessions: Monkey D, 0.92 ± 0.008 [95% CI]; Monkey C, 0.93 ± 0.013 [95% CI]). The effect of direct/indirect mapping on accuracy also vanished in the objective trials for Monkey D and was mitigated for Monkey C (across sessions: Monkey D: direct: 0.95 ± 0.012 [95% CI], indirect: 0.95 ± 0.014 [95% CI]; Monkey C: direct: 0.94 ± 0.02 [95% CI], indirect: 0.92 ± 0.013 [95% CI]).

To quantify the subjects' preference weightings for the two attributes, we fit choice data with a logistic regression model similar to those used in previous decision-making tasks (Conen & Padoa-Schioppa, 2019; Padoa-Schioppa & Assad, 2008). The model predicted choices from the log ratio of the ordinal magnitudes of each attribute, the mapping of each attribute (direct/indirect), and the position index of each option on the task screen (see Methods). The magnitudes of both attributes strongly predicted choices in both subjects (Figure 2D), showing that monkeys tended to pick the option with higher sweetness and probability. They also weighted the attributes roughly equally, with a slight bias toward probability (Monkey D: Log(ProbA/ProbB) $\beta = 1.83$, Log(SwtA/SwtB) $\beta = 1.62$; Monkey C: Log(ProbA/ProbB), $\beta = 2.64$, Log(SwtA/SwtB) $\beta = 1.18$; all $ps < 1 \times 10^{-13}$; Figures A1–A2). In contrast, attribute mappings and location on the screen had minimal effect on choice. Monkey D showed a tendency to select options with indirect probability mappings in early testing sessions, but this disappeared over time (Figure A2). Therefore, monkeys primarily used sweetness and probability information to guide decisions. Choice RTs were also faster with larger differences in EV and larger differences in each attribute (Figure A3).

## Mapping Mismatches Impair Attribute Comparisons

Next, we considered two operations that could be involved in computing decisions: integrating attribute values within an option and directly comparing like attributes across the different options. Because it is relatively straightforward to identify a larger or smaller bar from a pair, these processes should be easier when bars have the same mapping and more difficult when they differ (i.e., when one is direct and one is indirect). If options are assessed solely on the basis of integrated value, the attributes need to be integrated into an overall value before comparison with another option. In this case, mismatching direct and indirect mappings "within an option"

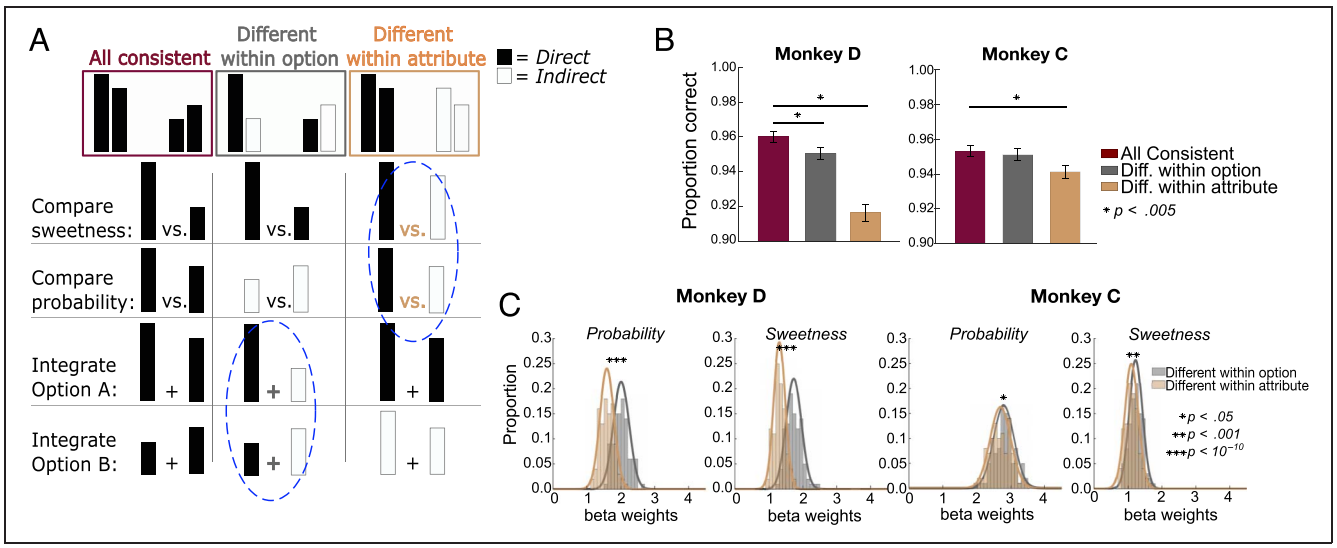


**Figure 3.** Choice accuracy varies with attribute arrangement. (A) Schematic of three trial types. Burgundy: All attributes have the same mapping, either all "direct" (shown) or all "indirect" (not shown). On these trials, comparison or integration processes would take place among attributes with the same mapping. Gray: Mappings differ among attributes within an option, but like attributes of the two options are the same. In this case, attribute comparisons would take place between bars with the same mapping, but integration within an option would take place across mismatched mappings (blue dashed circle). Gold: Mappings differ within like attributes but are the same within each option, so attribute comparisons would take place between mismatched mappings (blue dashed circle), but value integration would take place between bars with the same mapping. Note that, in the last two trial types, there are always two bars of each mapping, and only their arrangement differs. (B) Accuracy on trials of each type in which there was also an objectively better option ($n = 3728$ and 4188 trials for Monkeys D and C, respectively). Accuracy was consistently lower when like attributes differed (gold). *Significant post hoc comparisons, binomial test. Error bars indicate *SEM*. (C) Distributions of bootstrapped samples of 400 trials, sampled from all trials (not only those with an objectively better option) in which attribute mappings were different within option (gray) or different within attribute (gold) as in A. Mismatched mappings within attribute consistently resulted in smaller slopes (i.e., more variable choices). *Significant Wilcoxon rank-sum tests. Monkey D: $n = 57{,}082$; Monkey C: $n = 65{,}384$.

should disrupt the integration of the attributes and impair choice accuracy. Once the option values are computed, the original bar mapping should no longer matter, meaning that mismatches across options should not have the same effect. Conversely, if monkeys use direct attribute comparisons to compute a choice, then mismatched mappings "within like attributes" (across options) should impair choice accuracy (Figure 3A). Because attribute mappings varied independently, we were able to subselect trials where attributes were either matched or mismatched in different combinations to test these hypotheses.

First, we focused on trials with an objectively better option, as described above, so we could calculate choice accuracies. Among these trials, we compared accuracy when all four bars had a consistent mapping, meaning all were direct or all were indirect, to accuracies when two bars were direct and two were indirect. In the latter case, we separated trials in which like attributes had the same mapping but differed within an option and those in which the two bars of an option had the same mapping but differed from the two bars of the other option. On these trials, monkeys were consistently less accurate when bars of like attributes had mismatched mappings, suggesting a disruption of attribute-level comparisons [one-way ANOVA: Monkey D: $F(2, 10897) = 35.58$, $p = 3.97 \times 10^{-16}$; Monkey C: $F(2, 12595) = 3.48$, $p = .03$; Figure 3B]. In contrast, when options are matched within attribute but mismatched within option, we found less or no deficit in choice accuracy. Because there was the same number of direct or indirect attributes in each condition and attributes merely varied in arrangement, the slightly lower accuracy using indirect bars cannot explain this result. Likewise, mappings were randomly and independently assigned to each attribute and option, so the mapping of a particular attribute could not influence this effect. Instead, the arrangement of attribute mappings in the choice determined choice accuracy. Similar but more subtle effects were found in RTs (Figure A4).

To assess effects across all choices (not only objective ones), we separately modeled trials in which bar mappings differed within an option and those in which bars differed within like attributes as sigmoid functions (Equation 3). If different bar mappings impeded within-attribute comparisons, we would expect less consistent choices on those trials, quantified as shallower fitted slopes. To control for effects of trial number, we created 100 bootstrapped samples of 400 trials for each condition and estimated distributions of fitted slopes for each. We found that choices were more variable when bars differed within attribute versus within option for both sweetness and probability (Figure 3C). The effect was slightly stronger when models were fit only to trials without an objectively better option, compared to those where one option was better in both attributes (Figure A5). This was expected if the more difficult nonobjective trials were more taxing on comparison processes, therefore revealing stronger differences. Overall, preventing monkeys from easily making direct attribute comparisons resulted in less accurate choice behavior, suggesting that they rely on these comparisons to make multiattribute decisions.

### Gaze Patterns during Multiattribute Choices

As humans or monkeys decide, they acquire information by shifting gaze among visible options, and this process of allotting attention influences the dynamics of decision formation (Smith & Krajbich, 2019; Lim, O'Doherty, & Rangel, 2011; Armel, Beaumel, & Rangel, 2008). Our task presented attributes as physically separate bars, which allowed us to use eye tracking to quantify gaze patterns across the different options and attributes. First, we focused on fixations on attribute bars before a choice was made (the prechoice epoch). The final fixation that coincided with the choice report, when the monkey released the touch bar, was excluded. Monkey C made slightly fewer fixations per trial than Monkey D (Monkey D: mean = 2.89 fixations, $SE = 0.0058$, $n = 43{,}052$ trials; Monkey C: mean = 2.35 fixations, $SE = 0.0034$, $n = 38{,}781$ trials), and both monkeys exhibited idiosyncratic preferences for looking at either the sweetness (Monkey D) or probability (Monkey C) bars (Figure A6). Notably, despite these tendencies, behavioral choices reflected clear usage of information represented by both attribute bars (see Figure 2D). Therefore, gaze bias is not a one-to-one proxy for preference and is dissociable from choice behavior, although they are not entirely independent.

First, we determined whether there were general patterns that related gaze behavior to choices. Both monkeys made more fixations per choice as the difference between the attributes in the two options decreased, so they looked more at the options when choices were more difficult (i.e., close in value; Figure 4A). We quantified this with a general linear regression that predicted the number of fixations on any attribute bar from the difference in offered sweetnesses and probabilities, as well as the mapping of each attribute, and found that smaller differences in either attribute predicted more fixations per trial (Monkey D and C, respectively: sweetness difference: $\beta = -0.10$ and $-0.02$, $p = 2.71 \times 10^{-112}$ and $4.77 \times 10^{-10}$; probability difference: $\beta = -0.17$ and $-0.10$, $p = 8.8 \times 10^{-317}$ and $3.37 \times 10^{-297}$). In addition, consistent with previous reports (Krajbich et al., 2010), fixations were longer when monkeys looked at either bar of the option they would eventually select (the "chosen option"), compared to the one they would not (the "unchosen option"; Figure 4B). Therefore, aspects of the monkeys' gaze patterns aligned with expected effects of value and choice.

Next, we assessed effects of attribute mapping on gaze patterns. Here, Monkey D slightly preferred to look at indirect sweetness and probability bars, whereas Monkey C preferred to look at indirect sweetness bars but direct probability bars (Figure A6B). These patterns are reflected in the effects of bar mappings on fixation number in the

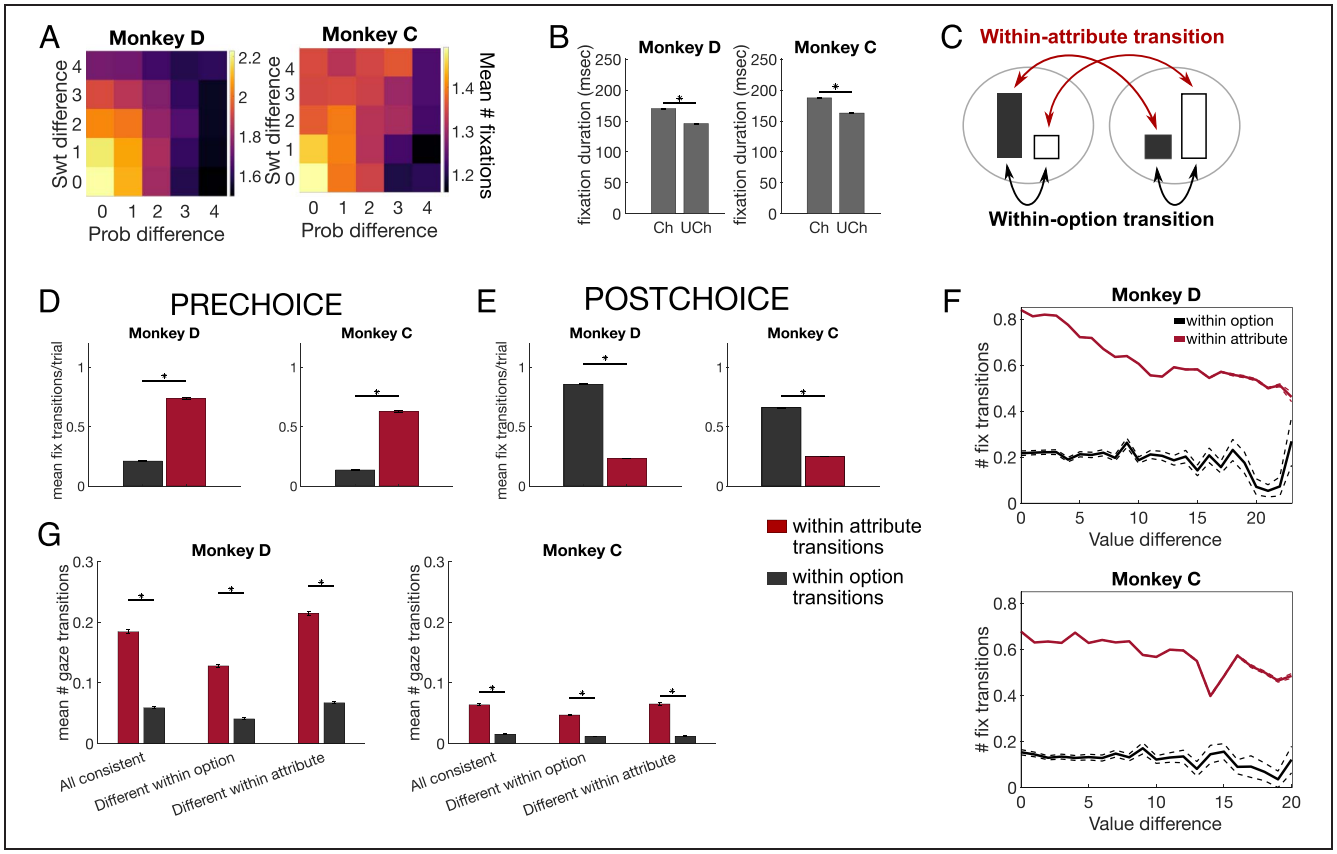


**Figure 4.** Gaze patterns in multiattribute choices. (A) Colormaps show that the mean number of fixations on any bar scaled with the ordinal difference between sweetness and probability of the choice options. Monkey D: $n$ = 51,115; Monkey C: $n$ = 53,727. (B) The mean duration of fixations on either bar of the chosen option (Ch) was higher than those on bars of the unchosen (Uch) option. Bars show the aggregate of all fixations in a trial, and error bars represent 99% confidence intervals. Monkey D: $n$ = 51,115 fixations; Monkey C: $n$ = 53,727 fixations. (C) Schematic showing within-attribute (red arrows) and within-option (black arrows) gaze transitions. Black bars represent sweetness, white bars represent probability, and an option comprises two bars in the same gray circle. (D) Number of fixation (fix) transitions within option (black) or within attribute (red) for each monkey before a choice is made. Error bars indicate *SEM*. *$p < 10^{-10}$. $n$ = 88,819 (Monkey D) and 106,800 (Monkey C) fixation transitions. (E) Number of fixation transitions as in D, except after the choice is reported. $n$ = 81,909 (Monkey D) and 110,400 (Monkey C) fixation transitions. (F) The number of fixation transitions per trial within option or within attribute varied with the difference in EV of the choice options on that trial. Dashed lines show *SEM* (very small because of a high number of trials). $n$ = 43,430 (Monkey D) and 27,055 (Monkey C) trials. (G) The number of fixation transitions per trial, split by attribute arrangement, as in Figure 2E. Planned post hoc comparisons from a two-way ANOVA compared within-attribute and within-option transitions. *$p < .0033$ (Bonferroni-corrected). Error bars indicate 95% CI. $n$ = 43,430 (Monkey D) and 27,055 (Monkey C) trials.

linear model (Monkey D and C: number of indirect sweetness bars: $\beta = 0.004$ and 0.05, $p = .57$ and $8.36 \times 10^{-32}$; number of indirect probability bars: $\beta = -0.06$ and $-0.11$, $p = 2.49 \times 10^{-18}$ and $5.41 \times 10^{-131}$), but effects are weak compared to the attribute magnitudes and idiosyncratic to the individual monkeys.

Finally, we assessed the same effects on fixation durations, using a linear regression model to predict the duration of any fixation from features of the fixated bar (magnitude and mapping), features of the nonfixated bars, and fixation sequence. Across monkeys, fixations were longer for probability bars, chosen options, indirect bars, and greater values of the fixated attribute (Figure A7). In addition, there were some effects of unfixated attributes. Both monkeys showed shorter fixations when either attribute of the other option had a greater value. However, for greater values of the other attribute of the same option, Monkey C had longer fixations, whereas Monkey D had shorter. Together, the strongest patterns in gaze behavior were related to the monkeys' choices, with only weak or idiosyncratic effects of other variables such as attribute mapping suggesting that gaze can provide a window into decision-making processes.

## Gaze Transitions Are Consistent with Attribute Comparison

Our choice data suggested that monkeys compared like attributes of the two options when making a decision. Gaze shifts can provide insights into the order of information sampling and therefore reveal patterns consistent with attribute comparison or value integration. If monkeys use direct comparison of attributes to help them decide, we predicted that most gaze transitions would be between bars representing like attributes. To assess this, we determined how often gaze transitioned between attributes of

the same option (i.e., sweetness bar A ↔ probability bar A, or sweetness bar B ↔ probability bar B), which would be expected during integration into an overall value. We compared this to transitions between two bars representing like attributes (i.e., sweetness bar A ↔ sweetness bar B, or probability bar A ↔ probability bar B), which would be expected with attribute comparisons (Figure 4C). For this analysis, trials with less than two fixations before a choice were excluded, yielding 22,357 (D) and 10,728 (C) trials for gaze transition analyses (for prechoice fixations) and 43,430 (D) and 32,046 (C) for postchoice analysis. Gaze transitions that were neither between like attributes nor between the two attributes of an option (e.g., sweetness bar A ↔ probability bar B) were also excluded.

Both subjects made significantly more within-attribute transitions than within-option transitions in the prechoice epoch [Monkey D: $t(36{,}378) = -86.1, p < 1 \times 10^{-13}$; Monkey C: $t(17{,}079) = -70.6, p < 1 \times 10^{-12}$; Figure 4D]. This is consistent with the idea that monkeys compare information about the like attributes to each other. As a follow-up, we quantified the same measure in the postchoice epoch, when only the chosen option was displayed on the screen. Despite the unchosen option not being visible, monkeys occasionally looked to the location where it previously was, but predominantly, we found within-option transitions as expected [Monkey D: $t(64{,}609) = 122.8, p < 1 \times 10^{-14}$; Monkey C: $t(58{,}684) = 91.456, p < 1 \times 10^{-13}$; Figure 4E]. In summary, monkeys showed within-attribute sampling of information before making a choice.

Next, we assessed how both types of gaze transitions changed with choice difficulty, using the difference in EVs between the two options as a proxy for the difficulty of the decision. Although both within-option and within-attribute transitions increased on more difficult trials, the increase in within-attribute transitions was greater than within-option transitions (Figure 4F). This was quantified by significantly greater slopes in a regression that correlated number of within-attribute gaze transitions and EV difference, compared to the same regression for within-option transitions [$t$ test for differences between slopes; Monkey D: $t(44{,}668) = -13.3, p < 1 \times 10^{-10}$; Monkey C: $t(21{,}342) = -3.57$, $p = 3.59 \times 10^{-4}$]. Therefore, within-attribute transitions predominate when choices are more difficult, which would be expected if these shifts in attention mediate comparison of like attributes.

Finally, we considered whether gaze transitions also reflected the perceptual difficulty of the decision by assessing trials where the bar mappings were (1) all consistent, (2) different within option, or (3) different within attribute, as in Figure 3A. Here, monkeys primarily made within-attribute gaze transitions, regardless of attribute arrangement. There was a significant interaction between categorical factors of Trial type (attribute mapping: all consistent, different within option, or different within attribute) and Transition type (within-attribute or within-option) on the number of fixation transitions per trial [two-way ANOVA; Monkey D: $F(2, 14777) = 5.64, p = .004$; Monkey C: $F(2, 12905) = 3.9, p = .02$]. This was driven by within-option transitions increasing proportionally more on different within-attribute trials (i.e., when mappings were consistent within option), although there were more within-attribute transitions on all trial types (Figure 4G). Therefore, in agreement with patterns in choice behavior, gaze behavior also indicated that monkeys used attribute comparisons to guide their choices. In addition, gaze patterns primarily reflected choice difficulty related to value difference but not perceptual difficulty.

### Simulations of Choice Behavior

Our behavior data indicate that monkeys use information about separate attributes to make value-based choices. However, this should be a suboptimal strategy in this task, if optimal choices are defined as the total EV of a series of choices. To assess the optimality of monkeys' choices, we quantified the EV of each option in terms of milligrams of sucrose, by multiplying the amount of sucrose in each option by the probability of receiving it. We then tested three models of choice behavior that differed in how they computed the values of options and determined the total amount of sucrose each would earn over a series of simulated trials. The first model calculated EVs as we defined them. The second computed the log ratio of each attribute, as in Figure 2D, and the third computed the difference among attributes, allowing each to be independently weighted (see Methods). The model based on log ratios of attributes (henceforth, Log model) is commonly used in choice tasks (Conen & Padoa-Schioppa, 2019; Padoa-Schioppa & Assad, 2006, 2008) and derived from the assumption that the two attributes are multiplicatively combined when calculating an option value, although they are independently weighted (Padoa-Schioppa, 2022). Therefore, the main difference between the Log model and the EV model is that attribute weights are free parameters in the Log model versus determined as a simple multiplication of milligrams times probability in the EV model. On the other hand, the Diff model assumes a linear rather than multiplicative combination of attributes and has been used to model choices among "bundles," or separate outcomes that must be chosen together (Padoa-Schioppa, 2022; FitzGerald, Seymour, & Dolan, 2009). In each case, we used logistic regression to fit a sigmoid to choices in the task, separately for each session, to obtain weights on each model predictor. We then tested the models on all 625 possible choices among different combinations of sweetness and probability. We found that, as expected, the EV model earns the greatest amount of sucrose overall [repeated-measures ANOVAs: Monkey D: $F(2, 136) = 154.5, p = 1 \times 10^{-27}$; Monkey C: $F(2, 152) = 343.6, p = 4.1 \times 10^{-57}$; Figure 5A]. However, model comparisons using AIC revealed that the Diff model was the better fit to each monkey's behavior [repeated-measures ANOVAs:

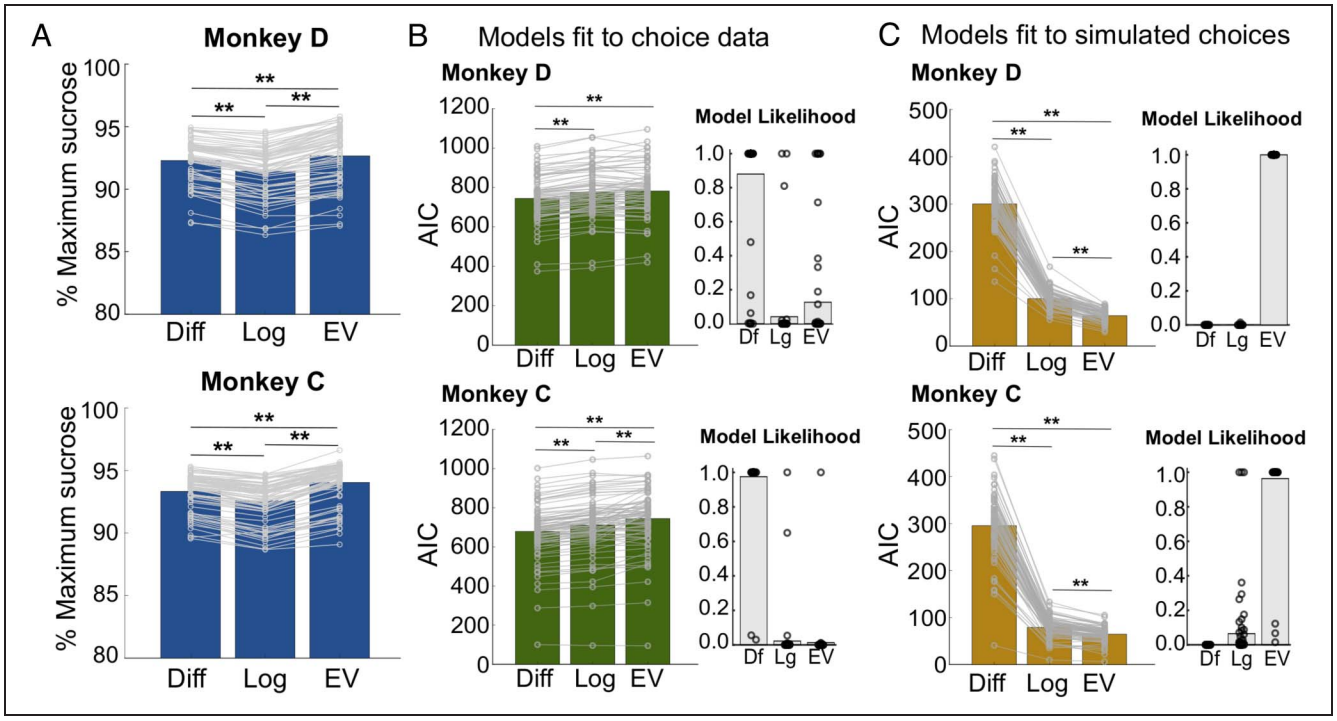


**Figure 5.** Models of multiattribute choice behavior. (A) EVs earned by each model, shown as the percentage of the maximum amount of sucrose that could be obtained, calculated across 625 trials consisting of all possible choices among combinations of sweetness and probability in the task. Models were fit to actual choice data on a session-by-session basis to obtain attribute weights. Bars = average, points = sessions. **Bonferroni-corrected post hoc comparisons, $p < 1 \times 10^{-3}$. (B) The fit of each model to the monkeys' choices was compared with AICs, computed for each session. Insets show the relative likelihood of each model for each session. Bars = average, points = sessions. **Bonferroni-corrected post hoc comparisons, $p < 1 \times 10^{-7}$. (C) Each model was fit to a pattern of "optimal" choices, or choices that would, on average, maximize the earned sucrose, and compared with AICs. Insets show the relative likelihood of each model for each session. Bars = average, points = sessions. **Bonferroni-corrected post hoc comparisons, $p < 1 \times 10^{-20}$. Df = Diff; Lg = Log.

Monkey D: $F(2, 136) = 69.7, p = 1.4 \times 10^{-21}$; Monkey C: $F(2, 152) = 121.58, p = 2.9 \times 10^{-32}$; Figure 5B]. This suggests that monkeys favored a decision strategy that is suboptimal in this task. Alternatively, their behavior could have been optimized for something other than total milligrams of sucrose, although they showed consistent preferences for sweeter, more probable options.

For comparison, we also fit the same three models to simulated trials in which options were drawn from actual trials, but simulated choices reflected the higher EV (in milligrams of sucrose) or a random selection on choices with equivalent EVs. In this case, the EV model was the best fit to the simulated choices [repeated-measures ANOVAs: Monkey D: $F(2, 136) = 2082.7, p = 9.9 \times 10^{-103}$; Monkey C: $F(2, 152) = 1461.3, p = 5.6 \times 10^{-100}$; Figure 5C]. The Log model was also a close fit, reflecting the fact that it differs from the EV model only in allowing attributes to be weighted, and in this case, the weights were fit to a pattern of choices consistent with a multiplicative EV computation. In contrast, the Diff model, which fit actual choice data the best, was the poorest fit when choices are based strictly on EVs. Together, these simulations support the notion that monkeys solve this multiattribute decision task using a strategy that involves consideration of individual attributes, rather than strictly computing an integrated EV.

## DISCUSSION

A central premise of most decision-making models is the idea that choices involve the computation and comparison of integrated values. However, other views have proposed that unintegrated attributes also play a role. Here, we used a novel multiattribute decision-making task for monkeys to test whether complex decisions incorporate information about unique attributes as part of the choice process. Patterns in choice accuracy, preference consistency, and directed gaze all indicated that monkeys spontaneously used direct comparisons of like attributes to arrive at a decision. Importantly, this occurred while information was also available to compute integrated values, so the task revealed aspects of the monkeys' natural tendency to use unintegrated attributes. Consistent with this, our simulations indicated that modeling the monkeys' choices with an EV computation fit their behavior patterns worse than choice models that parameterize the attributes independently. Although these data do not exclude a role for integrated value comparisons, they do emphasize that integrated value is not the sole decision variable that the brain uses when computing a preference-based choice. Because our experiment included only two young adult male monkeys, further studies will be needed to determine if this decision-making strategy is affected by biological variables such as age or sex.

Our results provide support for a class of model in which choices are based on evaluation of individual attributes, either without (Trueblood, Brown, & Heathcote, 2014; Hotaling, Busemeyer, & Li, 2010; Usher & McClelland, 2004; Roe et al., 2001) or in parallel to (Hunt & Hayden, 2017; Hunt et al., 2014) the computation of integrated values. Many models that include within-attribute comparisons also account for classic anomalies in multiattribute choices, such as context effects (Landry & Webb, 2021; Turner, Schley, Muller, & Tsetsos, 2018). For example, one type of model proposes that attributes are compared in a pairwise manner and evidence in favor of an option accumulates linearly, weighted by attention. This accounts for attraction effects because greater attentional weights are placed on options that are closer together in attribute space (Turner et al., 2018; Trueblood et al., 2014). In addition to our results, models such as this support the validity of attribute-based theories of decision-making.

Our results could also align with theories that propose decisions arise from parallel comparisons of multiple variables, including like attributes, integrated values, and attribute saliencies (Hunt et al., 2014; Cisek, 2012). From this view, decisions arise from distributed brain systems, which may be arranged hierarchically, such that information about option and attribute values can be jointly used along with other variables to produce a decision (Hunt et al., 2014). Notably, our study cannot address situations where options do not share a common attribute. Whereas some have proposed that this is a context in which integrated value comparisons are particularly important (Padoa-Schioppa, 2011), other models solve this dilemma with a series of accept/reject decisions at the level of attributes (Stewart et al., 2006). Regardless, our results demonstrate the need to consider attribute-level processes as a mechanism involved in multiattribute decision-making.

Our conclusions are based in part on subtle impairments in choice behavior revealed by our task design, which incorporated different perceptual mappings of visual cues to attribute values (i.e., "bigger is better" vs. "smaller is better"). When mappings of two attribute bars were the same, the monkeys could compare them with a simple perceptual judgment to determine which is taller or shorter, or they could reference internal representations of either the specific meaning (e.g., 50% probability of reward) or the position on a value scale indicated by each bar. When the mappings differed, however, they could not use simple perceptual judgments and had to rely on and translate between internal representations, making the mismatched condition potentially more difficult. Indeed, we found lower objective accuracies and less consistent preferences when mappings were different within like attributes, suggesting that like attributes were the components of the display that the monkeys were translating between.

Having the same mapping not only provides an easier way of comparing bars but also can be seen as grouping them, either perceptually (by color) or informationally (by relationship of size to goodness). Previous work has shown that grouping attributes by type or the option they belong to, either through colored backgrounds or proximity, without introducing significant processing costs, does not change decision-making strategies (Ettlin & Bröder, 2015). This makes it unlikely that the perceptual grouping drove our behavioral effects. Rather, our data suggest that an inefficiency was introduced to the decision process when the subjects had to compare attributes across informational groups (i.e., different mappings). Because the same degree of deficit was not seen when there were discordant informational groups within an option, it suggests that operations taking place within an option are less critical to the choice process, and the brain relies more on direct attribute comparison to make decisions.

It is unlikely that our behavioral effects were driven by perceptual features in other ways, for instance, by way of differences in preference or accuracy of value estimation for one of the mappings. This is because we subselected trials from our large data set that had an identical number of "direct" and "indirect" bars on the screen in each condition (i.e., different within option or different within attribute). With this approach, only the particular arrangement of the matched or mismatched attributes varied across conditions, eliminating effects that might arise merely from the monkeys' interpretations of the direct or indirect condition.

If monkeys used comparison of attributes to help them make decisions, we expected this would also be evident in the way they gathered information while making a choice. For this, we analyzed patterns of fixation and predicted that gaze would predominantly transition between the bars representing like attributes. From this view, shifting gaze reflects a process by which items are brought into the focus of attention and therefore sequentially sampled (Krajbich et al., 2010). As predicted, we found a tendency to shift gaze between like attributes, particularly on more difficult choices when the options were more similar in value. This is consistent with human studies, which find that gaze tends to shift primarily between alternatives along single attribute dimensions during multiattribute choices (Ryan-Lortie, Pelletier, Pilgrim, & Fellows, 2023; Noguchi & Stewart, 2014; Russo & Rosen, 1975). It is also in line with lesion evidence indicating the importance of sampling attributes in sequence in choice behavior. For instance, when asked to choose between hypothetical apartments that vary in multiple features, control subjects tended to favor attribute-based strategies and uncovered information about like attributes in sequence (Fellows, 2006). In contrast, individuals with damage to the ventromedial PFC, an area important for value-based decision-making, tended to favor alternative-based decision strategies, seeking out all of the information pertaining to a given option at once. This suggests that damage to decision-making circuits disrupted an otherwise common tendency to sequentially gather information about like attributes. Therefore, across species, gaze patterns

consistently reveal preferences for within-attribute gaze transitions, reflecting a search strategy oriented toward making within-attribute comparisons.

Because the same decision can be made a number of different ways and can rely to varying degrees on unobservable internal states, studies often seek a fuller understanding of decision processes by assessing the neural substrates (Padoa-Schioppa, 2007). A number of brain regions have been implicated in value-based decision-making. Among these, the OFC is particularly important, as damage or disruption consistently alters value-based choice behavior, suggesting that OFC neurons perform choice-relevant computations (Ballesta, Shi, Conen, & Padoa-Schioppa, 2020; Rudebeck, Saunders, Prescott, Chau, & Murray, 2013). Integrated value signals are commonly found within OFC, including in single-unit firing rates (Padoa-Schioppa & Assad, 2006; Wallis & Miller, 2003; Tremblay & Schultz, 1999), population codes (Yamada et al., 2021; Rich & Wallis, 2016), field potentials (Saez et al., 2018; Rich & Wallis, 2016, 2017), and fMRI BOLD signals (Chikazoe, Lee, Kriegeskorte, & Anderson, 2014; Plassmann, O'Doherty, & Rangel, 2007), and this has been taken as evidence that integrated value is the key decision variable in OFC. However, multiple laboratories consistently report neurons in monkey OFC (primarily Area 13) that encode the value of unique attributes (Pastor-Bernier, Stasiak, & Schultz, 2019; Setogawa et al., 2019; Blanchard, Hayden, & Bromberg-Martin, 2015; Raghuraman & Padoa-Schioppa, 2014; Hosokawa, Kennerley, Sloan, & Wallis, 2013; Padoa-Schioppa & Assad, 2006), and similar signals can be found in human fMRI BOLD (Howard, Gottfried, Tobler, & Kahnt, 2015). These responses are understudied compared to the more prevalent integrated value signals, making it unclear whether they inform choice behavior or are used to compute the integrated values that then guide choice. On the basis of our results, the possibility of attribute-level processing should be considered when interpreting neural correlates of choice behavior in OFC and other regions.

In summary, our results provide robust behavioral evidence that monkeys use attribute comparisons when making multiattribute decisions. This stands in contrast to models in which choices emerge exclusively from the computation and comparison of integrated values and instead supports those that rely at least in part on attribute-level operations. This is particularly relevant when interpreting neural responses in choice paradigms where decision variables, such as attribute values and integrated values, are often correlated. Without directly testing alternate possibilities, the same data could be interpreted as support for entirely different psychological and neural mechanisms of decision-making.

## APPENDIX

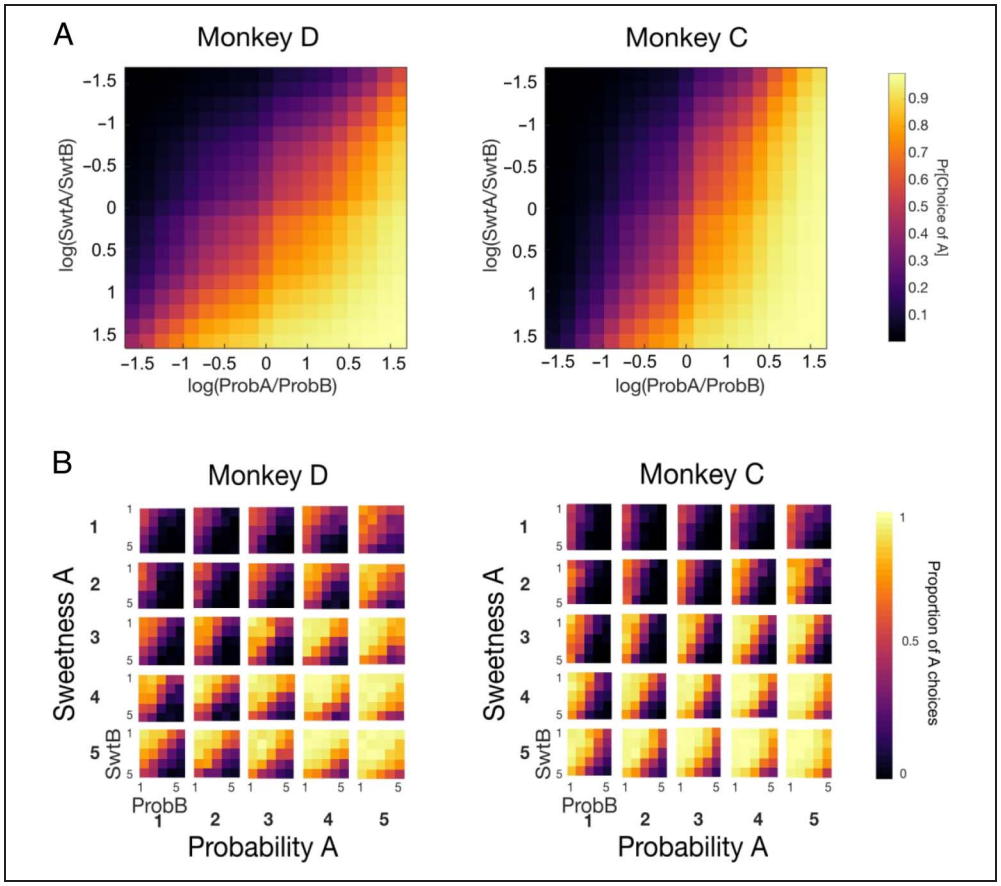


**Figure A1.** Monkeys use multiple attributes to make choices. (A) Colormap of predicted choice probabilities from logistic regression on the log ratio of Sweetness A/B and Probability A/B (as in Figure 2D, but flattened; Equation 3). Brighter colors represent greater frequency with which arbitrary option A was selected. $n$ = 57,082 (Monkey D) and 65,384 (Monkey C). (B) Colormaps of real choice frequencies. Each subplot shows choices when option A has sweetness magnitude of 1–5 (subplots from top to bottom, $y$ axis) and probability magnitude of 1–5 (subplots left to right, $x$ axis). Within each subplot, magnitudes of option B vary in the same range (1–5 for each). SwtB/ProbB = sweetness/probability of option B.

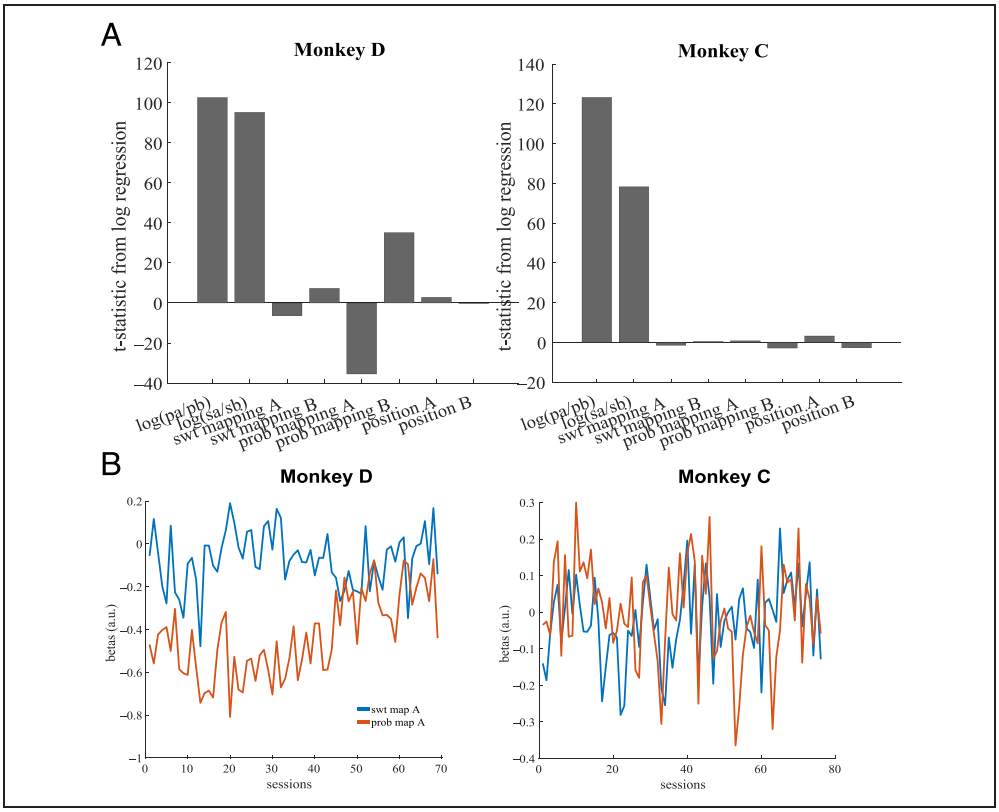


**Figure A2.** Regression coefficients from logistic regressions on choice. (A) Regressions performed on concatenated data (Equation 1) found that the strongest predictors of choice are the relative magnitude of sweetness and probability of the two options. $n$ = 57,082 (Monkey D) and 65,384 (Monkey C). (B) Plot of regression coefficients for sweetness/probability mapping from the choice regression over sessions. Only mapping betas for option A are shown, as betas for A and B are roughly inverses of each other. Across sessions, the relative weighting of direct versus indirect mapping varied considerably. Monkey D initially preferred indirect probability mappings, but this preference disappeared by the end of testing. Monkey C showed no consistent preference for direct or indirect mappings across testing.

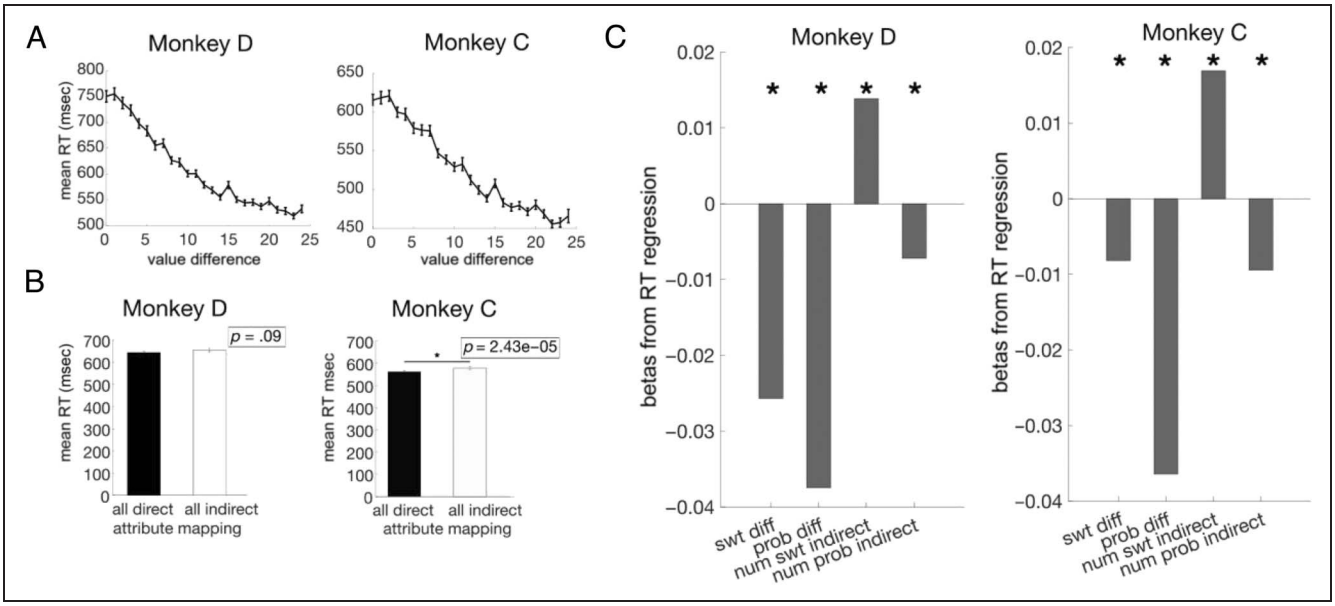


**Figure A3.** RTs in multiple attribute choices. RTs were defined as the time between the appearance of choice options on the screen and the time when the touch bar was released to select an option. Average RTs across sessions were 672.20 ± 30.5 msec for Monkey D and 570.31 ± 23.2 msec (95% CI) for Monkey C. RTs were shorter on trials with an objectively better option, compared to other trials, consistent with the idea that these are easier choices (Monkey D: 609.93 ± 11.68 msec [95% CI], Monkey C: 528.27 ± 10.33 msec [95% CI]; two-sample $t$ tests: Monkey D: $p = 7.93 \times 10^{-27}$, Monkey C: $p = 8.29 \times 10^{-40}$). (A) Average RTs across sessions varied with the difference in the EV of the two options, defined as the Ordinal Sweetness × Ordinal Probability. Error bars indicate *SEM*. $n$ = 69 (Monkey D) and 76 (Monkey C; sessions). (B) RTs were only weakly sensitive to direct/indirect attribute mapping in Monkey C (two-sample $t$ test). Error bars indicate *SEM*. $n$ = 69 (Monkey D) and 76 (Monkey C) sessions. (C) Regression coefficients from a linear regression on RT. SwtDiff and ProbDiff are the differences between the ordinal value of each attribute (0–4). NumSwtInd and NumProbInd are the number of indirect mappings of each attribute in the trial (0–2). *$p < 0.01$. $n$ = 56,889 (Monkey D) and 65,322 (Monkey C).

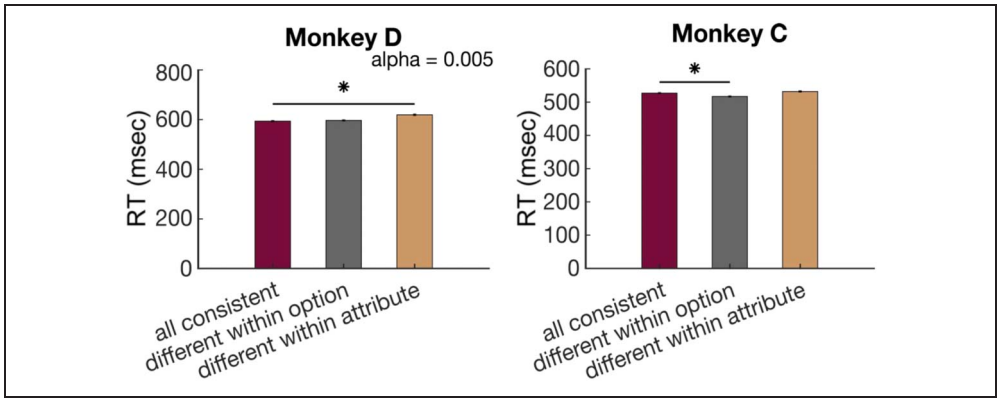


**Figure A4.** RTs split by attribute arrangement (as in Figure 2E). Error bars indicate *SEM*. Statistics were performed on log-transformed RTs. One-way ANOVA: Monkey D: $F(2, 10876) = 22.07, p = 2.71 \times 10^{-10}$; Monkey C: $F(2, 12586) = 14.11, p = 7.56 \times 10^{-7}$. Post hoc comparisons, $\alpha = .005$; Monkey D: all consistent versus different within option: $p = 0.98$, all consistent versus different within attribute: $p = 4.77 \times 10^{-9}$; Monkey C: all consistent versus different within option, $p = 2.92 \times 10^{-4}$, all consistent versus different within attribute, $p = .11$. Because of the sample size, some comparisons reached significance, but the effect size is very small and may reflect spurious effects.

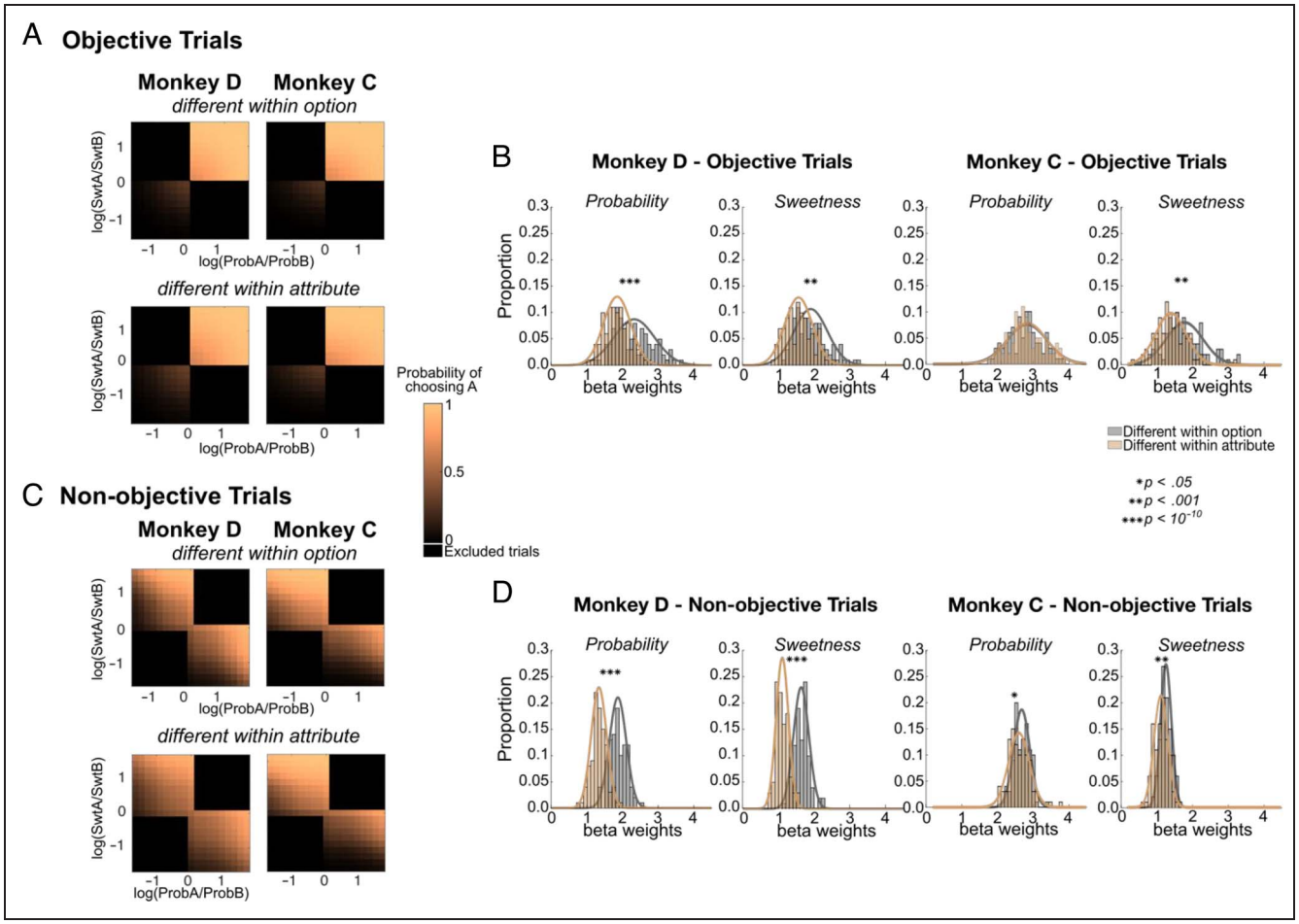


**Figure A5.** Choice models of objective and nonobjective trials. We compared trials with objectively better options ("Objective Trials") and those in which option A was better in one attribute and option B was better in the other ("Nonobjective Trials"). (A) Predicted probabilities from models fit to objective trials in which attributes were either mismatched within option (top) or within like attributes (bottom). Black regions indicate trials that were excluded because they did not meet the criteria of having one option superior to the other in both attributes. Monkey D: 18,207 included trials, Monkey C: 21,066 included trials. (B) Distributions of 100 bootstrapped samples of 400 trials, drawn from trials shown in A, in which attribute mappings were different within option (gray) or different within attribute (gold). Mismatched mappings within attribute consistently resulted in smaller slopes (i.e., more variable choices). (C) Predicted probabilities from models fit to nonobjective trials in which attributes were either mismatched within option (top) or within like attributes (bottom). Black regions indicate trials that were not included in the analysis because they did not meet these criteria. Monkey D: 38,875 included trials, Monkey C: 44,318 included trials. (D) Distributions of 100 bootstrapped samples of 400 trials, drawn from trials shown in C, separated as in B. Overall, there were slightly larger effects of attribute mapping on nonobjective trials, which may be more difficult for the monkey and therefore reveal choice inefficiencies to a greater extent. Importantly, all effects in any trial subset consistently showed that mismatched mappings within attribute resulted in smaller slopes (i.e., more variable choices). *Significant Wilcoxon rank-sum tests.

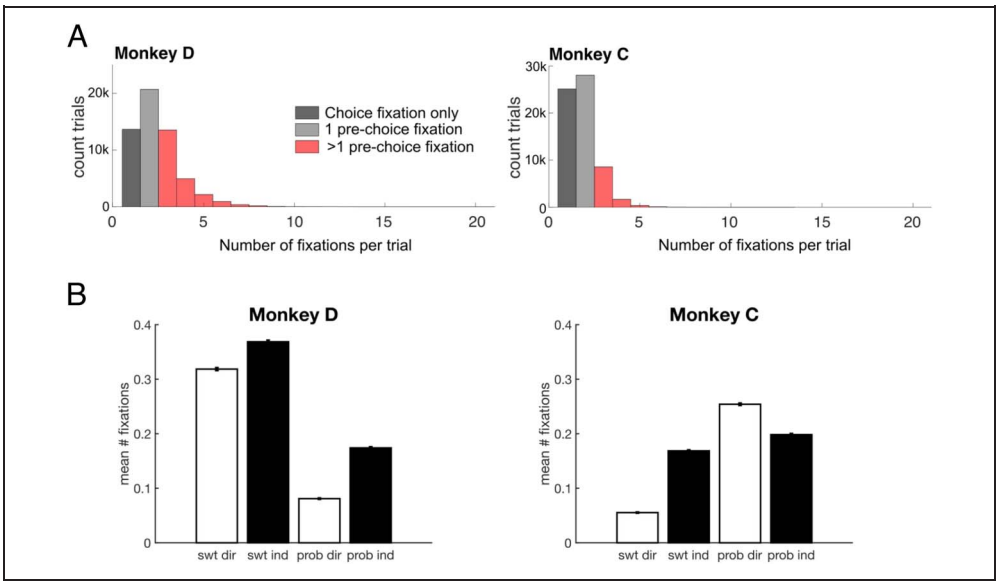


**Figure A6.** Number of fixations on attribute bars within a trial. (A) Histogram of number of fixations per trial. Fixations that coincided with the choice (dark gray) were removed from all analyses. Trials with less than two fixations (light gray) were removed from analyses of prechoice gaze transitions. (B) Mean number of fixations per trial, split by direct/indirect mapping of each attribute. Fixations were counted between cue onset and choice. Error bars indicate *SEM*. $n$ = 51,115 (Monkey D) and 53,727 (Monkey C) trials.

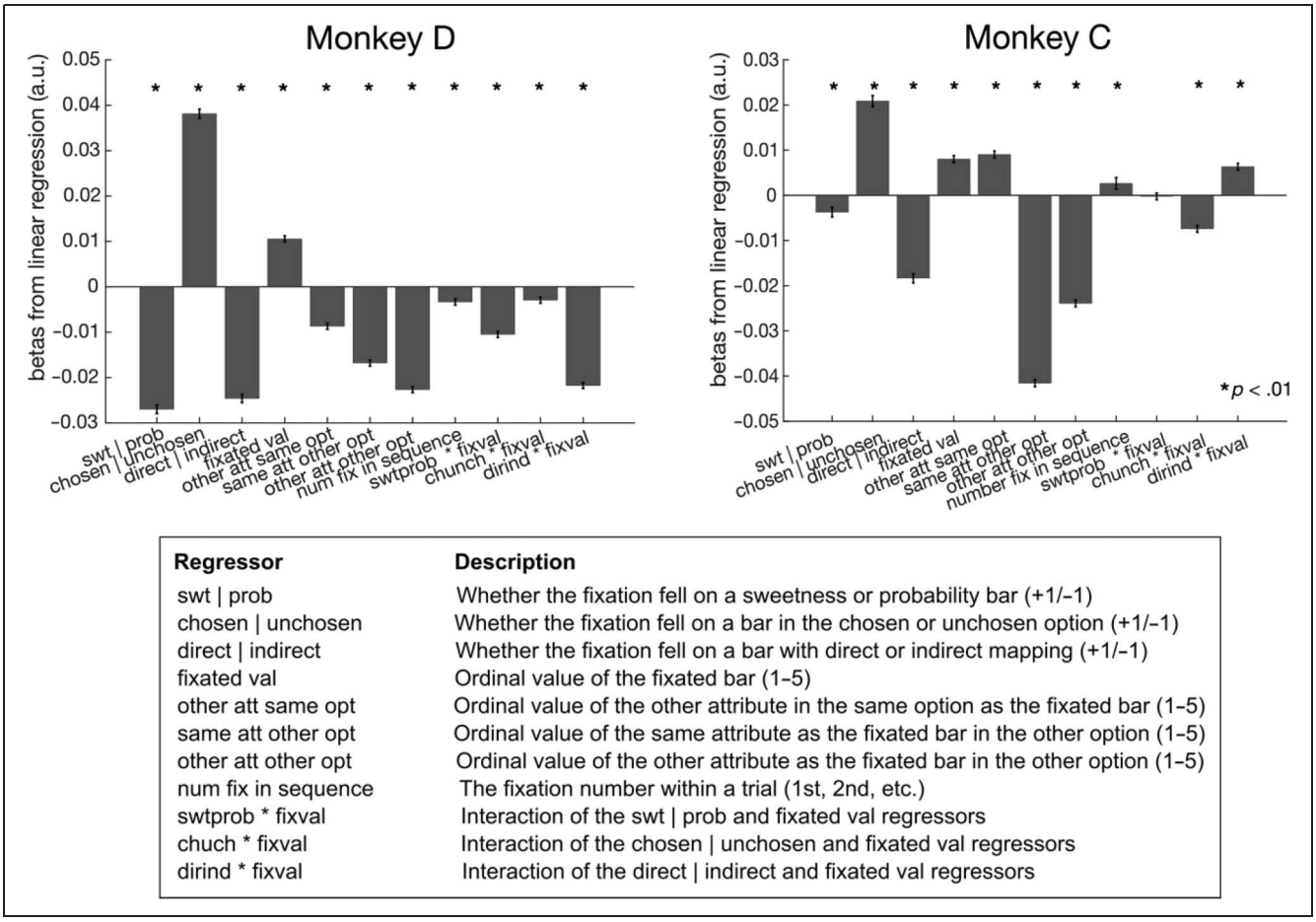


| Regressor | Description |
|---|---|
| swt \| prob | Whether the fixation fell on a sweetness or probability bar (+1/–1) |
| chosen \| unchosen | Whether the fixation fell on a bar in the chosen or unchosen option (+1/–1) |
| direct \| indirect | Whether the fixation fell on a bar with direct or indirect mapping (+1/–1) |
| fixated val | Ordinal value of the fixated bar (1–5) |
| other att same opt | Ordinal value of the other attribute in the same option as the fixated bar (1–5) |
| same att other opt | Ordinal value of the same attribute as the fixated bar in the other option (1–5) |
| other att other opt | Ordinal value of the other attribute as the fixated bar in the other option (1–5) |
| num fix in sequence | The fixation number within a trial (1st, 2nd, etc.) |
| swtprob * fixval | Interaction of the swt \| prob and fixated val regressors |
| chuch * fixval | Interaction of the chosen \| unchosen and fixated val regressors |
| dirind * fixval | Interaction of the direct \| indirect and fixated val regressors |

**Figure A7.** Regression coefficients from multiple linear regressions. Regressions predicted fixation duration (log[msec]) from predictor variables on the $x$ axis. *$p < .01$. Error bars show standard error of the coefficients. Ordinal values in the table are before mean centering. $n$ = 81,158 (Monkey D) and 52,416 (Monkey C) fixations.

## Acknowledgments

We thank Mark Baxter, Peter Rudebeck, and Feng-Kuei Chiang for their comments on the article.

Corresponding author: Erin L. Rich, One Gustave Levy Place Box 1639, New York, NY 10029, United States, or via e-mail: erin.rich@mssm.edu.

## Data Availability Statement

Behavioral data can be provided by the authors, pending scientific review. Requests for data should be submitted to the corresponding author.

## Author Contributions

Aster Q. Perkins: Data curation; Formal analysis; Funding acquisition; Investigation; Methodology; Software; Validation; Visualization; Writing—Original draft; Writing—Review & editing. Zachary S. Gillis: Conceptualization; Data curation; Investigation; Methodology; Software; Validation. Erin L. Rich: Conceptualization; Formal analysis; Funding acquisition; Methodology; Project Administration; Resources; Supervision; Validation; Writing—Original draft; Writing—Review & editing.

## Funding Information

National Institutes of Health grant R01MH134845 (E. L. R.). Pew Biomedical Scholars Program (E. L. R.). National Institutes of Health NRSA fellowship F31MH127901 (A. Q. P.).

## Diversity in Citation Practices

Retrospective analysis of the citations in every article published in this journal from 2010 to 2021 reveals a persistent pattern of gender imbalance: Although the proportions of authorship teams (categorized by estimated gender identification of first author/last author) publishing in the *Journal of Cognitive Neuroscience* (*JoCN*) during this period were M(an)/M = .407, W(oman)/M = .32, M/W = .115, and W/W = .159, the comparable proportions for the articles that these authorship teams cited were M/M = .549, W/M = .257, M/W = .109, and W/W = .085 (Postle and Fulvio, *JoCN*, 34:1, pp. 1–3). Consequently, *JoCN* encourages all authors to consider gender balance explicitly when selecting which articles to cite and gives them the opportunity to report their article's gender citation balance.

## REFERENCES

Armel, K. C., Beaumel, A., & Rangel, A. (2008). Biasing simple choices by manipulating relative visual attention. *Judgment and Decision Making*, *3*, 396–403. https://doi.org/10.1017/S1930297500000413

Asaad, W. F., Santhanam, N., McClellan, S., & Freedman, D. J. (2013). High-performance execution of psychophysical tasks with complex visual stimuli in MATLAB. *Journal of Neurophysiology*, *109*, 249–260. https://doi.org/10.1152/jn.00527.2012, PubMed: 23034363

Ballesta, S., Shi, W., Conen, K. E., & Padoa-Schioppa, C. (2020). Values encoded in orbitofrontal cortex are causally related to economic choices. *Nature*, *588*, 450–453. https://doi.org/10.1038/s41586-020-2880-x, PubMed: 33139951

Basten, U., Biele, G., Heekeren, H. R., & Fiebach, C. J. (2010). How the brain integrates costs and benefits during decision making. *Proceedings of the National Academy of Sciences, U.S.A.*, *107*, 21767–21772. https://doi.org/10.1073/pnas.0908104107, PubMed: 21118983

Berg, D. J., Boehnke, S. E., Marino, R. A., Munoz, D. P., & Itti, L. (2009). Free viewing of dynamic stimuli by humans and monkeys. *Journal of Vision*, *9*, 19–19. https://doi.org/10.1167/9.5.19, PubMed: 19757897

Blanchard, T. C., Hayden, B. Y., & Bromberg-Martin, E. S. (2015). Orbitofrontal cortex uses distinct codes for different choice attributes in decisions motivated by curiosity. *Neuron*, *85*, 602–614. https://doi.org/10.1016/j.neuron.2014.12.050, PubMed: 25619657

Brandstätter, E., Gigerenzer, G., & Hertwig, R. (2006). The priority heuristic: Making choices without trade-offs. *Psychological Review*, *113*, 409–432. https://doi.org/10.1037/0033-295X.113.2.409, PubMed: 16637767

Busemeyer, J. R., & Townsend, J. T. (1993). Decision field theory. *Psychological Review*, *100*, 432–459. https://doi.org/10.1037/0033-295X.100.3.432, PubMed: 8356185

Chau, B. K. H., Kolling, N., Hunt, L. T., Walton, M. E., & Rushworth, M. F. S. (2014). A neural mechanism underlying failure of optimal choice with multiple alternatives. *Nature Neuroscience*, *17*, 463–470. https://doi.org/10.1038/nn.3649

Chau, B. K., Law, C.-K., Lopez-Persem, A., Klein-Flügge, M. C., & Rushworth, M. F. (2020). Consistent patterns of distractor effects during decision making. *eLife*, *9*, e53850. https://doi.org/10.7554/eLife.53850, PubMed: 32628109

Chikazoe, J., Lee, D. H., Kriegeskorte, N., & Anderson, A. K. (2014). Population coding of affect across stimuli, modalities and individuals. *Nature Neuroscience*, *17*, 1114–1122. https://doi.org/10.1038/nn.3749

Cisek, P. (2012). Making decisions through a distributed consensus. *Current Opinion in Neurobiology*, *22*, 927–936. https://doi.org/10.1016/j.conb.2012.05.007, PubMed: 22683275

Conen, K. E., & Padoa-Schioppa, C. (2019). Partial adaptation to the value range in the macaque orbitofrontal cortex. *Journal of Neuroscience*, 2279–2218. https://doi.org/10.1523/JNEUROSCI.2279-18.2019, PubMed: 30833513

Ettlin, F., & Bröder, A. (2015). Perceptual grouping does not affect multi-attribute decision making if no processing costs are involved. *Acta Psychologica*, *157*, 30–43. https://doi.org/10.1016/j.actpsy.2015.02.002

Fellows, L. K. (2006). Deciding how to decide: Ventromedial frontal lobe damage affects information acquisition in multi-attribute decision making. *Brain*, *129*, 944–952. https://doi.org/10.1093/brain/awl017, PubMed: 16455794

Fisher, G. (2017). An attentional drift diffusion model over binary-attribute choice. *Cognition*, *168*, 34–45. https://doi.org/10.1016/j.cognition.2017.06.007

Fisher, G. (2021). A multiattribute attentional drift diffusion model. *Organizational Behavior and Human Decision Processes*, *165*, 167–182. https://doi.org/10.1016/j.obhdp.2021.04.004

FitzGerald, T. H. B., Seymour, B., & Dolan, R. J. (2009). The role of human orbitofrontal cortex in value comparison for incommensurable objects. *Journal of Neuroscience*, *29*, 8388–8395. https://doi.org/10.1523/JNEUROSCI.0717-09.2009, PubMed: 19571129

Glimcher, P. W., Dorris, M. C., & Bayer, H. M. (2005). Physiological utility theory and the neuroeconomics of choice. *Games and Economic Behavior*, *52*, 213–256. https://doi.org/10.1016/j.geb.2004.06.011, PubMed: 16845435

Gluth, S., Kern, N., Kortmann, M., & Vitali, C. L. (2020). Value-based attention but not divisive normalization influences decisions with multiple alternatives. *Nature Human Behaviour*, *4*, 634–645. https://doi.org/10.1038/s41562-020-0822-0, PubMed: 32015490

Gluth, S., Spektor, M. S., & Rieskamp, J. (2018). Value-based attentional capture affects multi-alternative decision making. *eLife*, *7*, e39659. https://doi.org/10.7554/eLife.39659, PubMed: 30394874

Hosokawa, T., Kennerley, S. W., Sloan, J., & Wallis, J. D. (2013). Single-neuron mechanisms underlying cost–benefit analysis in frontal cortex. *Journal of Neuroscience*, *33*, 17385–17397. https://doi.org/10.1523/JNEUROSCI.2221-13.2013, PubMed: 24174671

Hotaling, J. M., Busemeyer, J. R., & Li, J. (2010). Theoretical developments in decision field theory: Comment on Tsetsos, Usher, and Chater (2010). *Psychological Review*, *117*, 1294–1298. https://doi.org/10.1037/a0020401, PubMed: 21038981

Howard, J. D., Gottfried, J. A., Tobler, P. N., & Kahnt, T. (2015). Identity-specific coding of future rewards in the human orbitofrontal cortex. *Proceedings of the National Academy of Sciences, U.S.A.*, *112*, 5195–5200. https://doi.org/10.1073/pnas.1503550112, PubMed: 25848032

Huber, J., Payne, J. W., & Puto, C. (1982). Adding asymmetrically dominated alternatives: Violations of regularity and the similarity hypothesis. *Journal of Consumer Research*, *9*, 90. https://doi.org/10.1086/208899

Hunt, L. T., Behrens, T. E., Hosokawa, T., Wallis, J. D., & Kennerley, S. W. (2015). Capturing the temporal evolution of choice across prefrontal cortex. *eLife*, *4*, e11945. https://doi.org/10.7554/eLife.11945, PubMed: 26653139

Hunt, L. T., Dolan, R. J., & Behrens, T. E. J. (2014). Hierarchical competitions subserving multi-attribute choice. *Nature Neuroscience*, *17*, 1613–1622. https://doi.org/10.1038/nn.3836, PubMed: 25306549

Hunt, L. T., & Hayden, B. Y. (2017). A distributed, hierarchical and recurrent framework for reward-based choice. *Nature Reviews Neuroscience*, *18*, 172–182. https://doi.org/10.1038/nrn.2017.7, PubMed: 28209978

Hunt, L. T., Kolling, N., Soltani, A., Woolrich, M. W., Rushworth, M. F. S., & Behrens, T. E. J. (2012). Mechanisms underlying cortical activity during value-guided choice. *Nature Neuroscience*, *15*, 470–476. https://doi.org/10.1038/nn.3017

Hunt, L. T., Malalasekera, W. M. N., de Berker, A. O., Miranda, B., Farmer, S. F., Behrens, T. E. J., et al. (2018). Triple dissociation of attention and decision computations across prefrontal cortex. *Nature Neuroscience*, *21*, 1471–1481. https://doi.org/10.1038/s41593-018-0239-5, PubMed: 30258238

Hwang, J., Mitz, A. R., & Murray, E. A. (2019). NIMH MonkeyLogic: Behavioral control and data acquisition in MATLAB. *Journal of Neuroscience Methods*, *323*, 13–21. https://doi.org/10.1016/j.jneumeth.2019.05.002, PubMed: 31071345

Jocham, G., Hunt, L. T., Near, J., & Behrens, T. E. J. (2012). A mechanism for value-guided choice based on the excitation–inhibition balance in prefrontal cortex. *Nature Neuroscience*, *15*, 960–961. https://doi.org/10.1038/nn.3140, PubMed: 22706268

Kahneman, D., & Tversky, A. (1979). Prospect theory: An analysis of decision under risk. *Econometrica*, *47*. https://doi.org/10.1142/9789814417358_0006

Krajbich, I., Armel, C., & Rangel, A. (2010). Visual fixations and the computation and comparison of value in simple choice. *Nature Neuroscience*, *13*, 1292–1298. https://doi.org/10.1038/nn.2635, PubMed: 20835253

Krajbich, I., & Rangel, A. (2011). Multialternative drift-diffusion model predicts the relationship between visual fixations and choice in value-based decisions. *Proceedings of the National Academy of Sciences, U.S.A.*, *108*, 13852–13857. https://doi.org/10.1073/pnas.1101328108, PubMed: 21808009

Krassanakis, V., Filippakopoulou, V., & Nakos, B. (2014). EyeMMV toolbox: An eye movement post-analysis tool based on a two-step spatial dispersion threshold for fixation identification. *Journal of Eye Movement Research*, *7*, 1–10. https://doi.org/10.16910/jemr.7.1.1

Landry, P., & Webb, R. (2021). Pairwise normalization: A neuroeconomic theory of multi-attribute choice. *Journal of Economic Theory*, *193*, 53. https://doi.org/10.1016/j.jet.2021.105221

Lim, S.-L., O'Doherty, J. P., & Rangel, A. (2011). The decision value computations in the vmPFC and striatum use a relative value code that is guided by visual attention. *Journal of Neuroscience*, *31*, 13214–13223. https://doi.org/10.1523/JNEUROSCI.1246-11.2011, PubMed: 21917804

Louie, K., Khaw, M. W., & Glimcher, P. W. (2013). Normalization is a general neural mechanism for context-dependent decision making. *Proceedings of the National Academy of Sciences, U.S.A.*, *110*, 6139–6144. https://doi.org/10.1073/pnas.1217854110, PubMed: 23530203

McGinty, V. B., Rangel, A., & Newsome, W. T. (2016). Orbitofrontal cortex value signals depend on fixation location during free viewing. *Neuron*, *90*, 1299–1311. https://doi.org/10.1016/j.neuron.2016.04.045, PubMed: 27263972

Milosavljevic, M., Malmaud, J., Huth, A., Koch, C., & Rangel, A. (2010). The drift diffusion model can account for the accuracy and reaction time of value-based choices under high and low time pressure. *Judgment and Decision Making*, *5*, 437–449. https://doi.org/10.1017/S1930297500001285

Nelson, M. (2023). *myBinomTest(s,n,p,Sided)*. MATLAB Central File Exchange. https://www.mathworks.com/matlabcentral/fileexchange/24813-mybinomtest-s-n-p-sided.

Noguchi, T., & Stewart, N. (2014). In the attraction, compromise, and similarity effects, alternatives are repeatedly compared in pairs on single dimensions. *Cognition*, *132*, 44–56. https://doi.org/10.1016/j.cognition.2014.03.006, PubMed: 24762922

Padoa-Schioppa, C. (2007). Orbitofrontal cortex and the computation of economic value. *Annals of the New York Academy of Sciences*, *1121*, 232–253. https://doi.org/10.1196/annals.1401.011, PubMed: 17698992

Padoa-Schioppa, C. (2011). Neurobiology of economic choice: A good-based model. *Annual Review of Neuroscience*, *34*, 333–359. https://doi.org/10.1146/annurev-neuro-061010-113648, PubMed: 21456961

Padoa-Schioppa, C. (2022). Logistic analysis of choice data: A primer. *Neuron*, *110*, 1615–1630. https://doi.org/10.1016/j.neuron.2022.03.002, PubMed: 35334232

Padoa-Schioppa, C., & Assad, J. A. (2006). Neurons in the orbitofrontal cortex encode economic value. *Nature*, *441*, 223–226. https://doi.org/10.1038/nature04676, PubMed: 16633341

Padoa-Schioppa, C., & Assad, J. A. (2008). The representation of economic value in the orbitofrontal cortex is invariant for changes of menu. *Nature Neuroscience*, *11*, 95–102. https://doi.org/10.1038/nn2020, PubMed: 18066060

Pastor-Bernier, A., Stasiak, A., & Schultz, W. (2019). Orbitofrontal signals for two-component choice options comply with indifference curves of revealed preference theory. *Nature Communications*, *10*, 4885. https://doi.org/10.1038/s41467-019-12792-4, PubMed: 31653852

Perkins, A. Q., & Rich, E. L. (2021). Identifying identity and attributing value to attributes: Reconsidering mechanisms of preference decisions. *Current Opinion in Behavioral Sciences*, *41*, 98–105. https://doi.org/10.1016/j.cobeha.2021.04.019, PubMed: 36341022

Philiastides, M. G., Biele, G., & Heekeren, H. R. (2010). A mechanistic account of value computation in the human brain. *Proceedings of the National Academy of Sciences, U.S.A.*, *107*, 9430–9435. https://doi.org/10.1073/pnas.1001732107, PubMed: 20439711

Piantadosi, S. T., & Hayden, B. Y. (2015). Utility-free heuristic models of two-option choice can mimic predictions of utility-stage models under many conditions. *Frontiers in Neuroscience*, *9*, 105. https://doi.org/10.3389/fnins.2015.00105, PubMed: 25914613

Plassmann, H., O'Doherty, J., & Rangel, A. (2007). Orbitofrontal cortex encodes willingness to pay in everyday economic transactions. *Journal of Neuroscience*, *27*, 9984–9988. https://doi.org/10.1523/JNEUROSCI.2131-07.2007, PubMed: 17855612

Raghuraman, A. P., & Padoa-Schioppa, C. (2014). Integration of multiple determinants in the neuronal computation of economic values. *Journal of Neuroscience*, *34*, 11583–11603. https://doi.org/10.1523/JNEUROSCI.1235-14.2014, PubMed: 25164656

Rangel, A., & Hare, T. (2010). Neural computations associated with goal-directed choice. *Current Opinion in Neurobiology*, *20*, 262–270. https://doi.org/10.1016/j.conb.2010.03.001

Rich, E. L., & Wallis, J. D. (2016). Decoding subjective decisions from orbitofrontal cortex. *Nature Neuroscience*, *19*, 973–980. https://doi.org/10.1038/nn.4320, PubMed: 27273768

Rich, E. L., & Wallis, J. D. (2017). Spatiotemporal dynamics of information encoding revealed in orbitofrontal high-gamma. *Nature Communications*, *8*, 1139. https://doi.org/10.1038/s41467-017-01253-5, PubMed: 29074960

Roe, R. M., Busemeyer, J. R., & Townsend, J. T. (2001). Multialternative decision field theory: A dynamic connectionst model of decision making. *Psychological Review*, *108*, 370–392. https://doi.org/10.1037/0033-295X.108.2.370, PubMed: 11381834

Rudebeck, P. H., Saunders, R. C., Prescott, A. T., Chau, L. S., & Murray, E. A. (2013). Prefrontal mechanisms of behavioral flexibility, emotion regulation and value updating. *Nature Neuroscience*, *16*, 1140–1145. https://doi.org/10.1038/nn.3440, PubMed: 23792944

Russo, J. E., & Rosen, L. D. (1975). An eye fixation analysis of multialternative choice. *Memory & Cognition*, *3*, 267–276. https://doi.org/10.3758/BF03212910, PubMed: 21287072

Rustichini, A., & Padoa-Schioppa, C. (2015). A neuro-computational model of economic decisions. *Journal of Neurophysiology*, *114*, 1382–1398. https://doi.org/10.1152/jn.00184.2015, PubMed: 26063776

Ryan-Lortie, J., Pelletier, G., Pilgrim, M., & Fellows, L. K. (2023). Gaze differences in configural and elemental evaluation during multi-attribute decision-making. *Frontiers in Neuroscience*, *17*, 1167095. https://doi.org/10.3389/fnins.2023.1167095, PubMed: 37694112

Saez, I., Lin, J., Stolk, A., Chang, E., Parvizi, J., Schalk, G., et al. (2018). Encoding of multiple reward-related computations in transient and sustained high-frequency activity in human OFC. *Current Biology*, *28*, 2889–2899. https://doi.org/10.1016/j.cub.2018.07.045, PubMed: 30220499

Setogawa, T., Mizuhiki, T., Matsumoto, N., Akizawa, F., Kuboki, R., Richmond, B. J., et al. (2019). Neurons in the monkey orbitofrontal cortex mediate reward value computation and decision-making. *Communications Biology*, *2*, 126. https://doi.org/10.1038/s42003-019-0363-0, PubMed: 30963114

Simonson, I. (1989). Choice based on reasons: The case of attraction and compromise effects. *Journal of Consumer Research*, *16*, 158. https://doi.org/10.1086/209205

Smith, S. M., & Krajbich, I. (2019). Gaze amplifies value in decision making. *Psychological Science*, *30*, 116–128. https://doi.org/10.1177/0956797618810521, PubMed: 30526339

Stewart, N., Chater, N., & Brown, G. D. A. (2006). Decision by sampling. *Cognitive Psychology*, *53*, 1–26. https://doi.org/10.1016/j.cogpsych.2005.10.003

Sutton, R. S., & Barto, A. G. (2018). *Reinforcement learning, second edition: An introduction*. Cambridge, MA: MIT Press.

Tremblay, L., & Schultz, W. (1999). Relative reward preference in primate orbitofrontal cortex. *Nature*, *398*, 704–708. https://doi.org/10.1038/19525, PubMed: 10227292

Trueblood, J. S., Brown, S. D., & Heathcote, A. (2014). The multiattribute linear ballistic accumulator model of context effects in multialternative choice. *Psychological Review*, *121*, 179–205. https://doi.org/10.1037/a0036137, PubMed: 24730597

Turner, B. M., Schley, D. R., Muller, C., & Tsetsos, K. (2018). Competing theories of multialternative, multiattribute preferential choice. *Psychological Review*, *125*, 329–362. https://doi.org/10.1037/rev0000089, PubMed: 29265855

Usher, M., & McClelland, J. L. (2004). Loss aversion and inhibition in dynamical models of multialternative choice. *Psychological Review*, *111*, 757–769. https://doi.org/10.1037/0033-295X.111.3.757, PubMed: 15250782

Wallis, J. D., & Miller, E. K. (2003). Neuronal activity in primate dorsolateral and orbital prefrontal cortex during performance of a reward preference task. *European Journal of Neuroscience*, *18*, 2069–2081. https://doi.org/10.1046/j.1460-9568.2003.02922.x, PubMed: 14622240

Wallis, J. D., & Rich, E. L. (2011). Challenges of interpreting frontal neurons during value-based decision-making. *Frontiers in Neuroscience*, *5*, 124. https://doi.org/10.3389/fnins.2011.00124, PubMed: 22125508

Yamada, H., Imaizumi, Y., & Matsumoto, M. (2021). Neural population dynamics underlying expected value computation. *Journal of Neuroscience*, *41*, 1684–1698. https://doi.org/10.1523/JNEUROSCI.1987-20.2020

Yang, X., & Krajbich, I. (2022). A dynamic computational model of gaze and choice in multi-attribute decisions. *Psychological Review*, *130*, 52–70. https://doi.org/10.1037/rev0000350, PubMed: 35025570

Yiu, Y.-H., Aboulatta, M., Raiser, T., Ophey, L., Flanagin, V. L., Zu Eulenburg, P., et al. (2019). DeepVOG: Open-source pupil segmentation and gaze estimation in neuroscience using deep learning. *Journal of Neuroscience Methods*, *324*, 108307. https://doi.org/10.1016/j.jneumeth.2019.05.016, PubMed: 31176683

Zaiontz, C. (n.d.). Comparing the slopes for two independent samples. *Real Statistics Using Excel*. https://real-statistics.com/regression/hypothesis-testing-significance-regression-line-slope/comparing-slopes-two-independent-samples/.